UNIVERSIDADE ESTADUAL PAULISTA "JÚLIO DE MESQUITA FILHO"
INSTITUTO DE BIOCIÊNCIAS DE BOTUCATU

Curso de Graduação em Ciências Biológicas

MATHIAS RENNÓ CHAVES

Molecular Evolution of Tumor Suppressor Gene Promoters in Bats: Unraveling Peto's Paradox with Phylogenetic and TFBS Enrichment Studies

Evolução Molecular dos Promotores de Genes Supressores de Tumor em Morcegos: Desvendando o Paradoxo de Peto com Estudos Filogenéticos e de Enriquecimento de SLFT

Botucatu-SP
2024

Molecular Evolution of Tumor Suppressor Gene Promoters in Bats: Unraveling Peto's Paradox with Phylogenetic and TFBS Enrichment Studies

Evolução Molecular dos Promotores de Genes Supressores de Tumor em Morcegos: Desvendando o Paradoxo de Peto com Estudos Filogenéticos e de Enriquecimento de SLFT

Aluno: Mathias Rennó Chaves

Orientadora: Profa. Dra. Mariana Freitas Nery

Trabalho de conclusão de curso apresentado ao Instituto de Biociências, Universidade Estadual Paulista "Júlio de Mesquita Filho", Campus de Botucatu, para a obtenção do título de Bacharel em Ciências Biológicas.

FICHA CATALOGRÁFICA ELABORADA PELA SEÇÃO TÉC. AQUIS. TRATAMENTO DA INFORM.
DIVISÃO TÉCNICA DE BIBLIOTECA E DOCUMENTAÇÃO - CÂMPUS DE BOTUCATU - UNESP

BIBLIOTECÁRIA RESPONSÁVEL: ROSANGELA APARECIDA LOBO-CRB 8/7500

Chaves, Mathias Rennó.
Molecular evolution of tumor suppressor gene promoters in bats : unraveling peto's paradox with phylogenetic and tfbs enrichment studies / Mathias Rennó Chaves. - Botucatu, 2024

Trabalho de conclusão de curso (bacharelado - Ciências Biológicas) - Universidade Estadual Paulista (UNESP), Instituto de Biociências, Botucatu
Orientador: Mariana Freitas Nery
Capes: 20205007

1. Bats. 2. Câncer. 3. Evolution. 4. Promoters (Genetics).

Palavras-chave: Bat; Cancer; Evolution; Peto's paradox; Promoter.

Molecular Evolution of Tumor Suppressor Gene Promoters in Bats: Unraveling Peto's Paradox with Phylogenetic and TFBS Enrichment Studies

Chaves, Mathias Rennó[1]; Nery, Mariana Freitas[2]*.

[1] Dept. of Chemical and Biological Sciences, Institute of Biosciences of Botucatu, São Paulo State University, Distrito de Rubião Júnior, Rua Prof. Dr. Antonio Celso Wagner Zanin, 250 Botucatu/SP 18618-689

[2] Dept of Genetics, Evolution, Microbiology & Immunology, Institute of Biology, University of Campinas, Rua Monteiro Lobato, 255 Campinas/SP 13083-862

* marinery@unicamp.br; Tel.: + 55 21 3938-735

Resumo

Contexto: A prevalência de câncer varia significativamente entre os mamíferos, apesar do risco compartilhado de desenvolver a doença. O modelo multistágio de Doll-Armitage sugere que organismos maiores e com maior longevidade deveriam ter maiores riscos de câncer devido ao aumento das divisões celulares e à acumulação de mutações. No entanto, o Paradoxo de Peto destaca que as taxas de câncer entre espécies não correlacionam com a massa corporal ou a longevidade, indicando que espécies maiores e mais longevas podem ter evoluído mecanismos superiores de supressão tumoral. Os morcegos, com sua excepcional longevidade em relação ao tamanho corporal e altas taxas metabólicas, oferecem uma oportunidade única para estudar esses mecanismos. Este estudo investiga a evolução molecular das regiões promotoras de genes supressores de tumor (GST) em morcegos, focando na evolução dos sítios de ligação de fatores de transcrição (SLFT) dentro desses promotores e sua conservação ou aceleração evolutiva.

Resultados: Selecionamos 12 GSTs frequentemente mutados em análises pan-câncer e recuperamos as regiões de 1500 bp a montante dos locais de início da transcrição desses genes. Árvores filogenéticas foram geradas usando o IQ-TREE, e as taxas evolutivas das regiões promotoras foram analisadas com as ferramentas phyloFit e phylo-P. A análise de enriquecimento de SLFT foi conduzida usando o software Ciiider. A maioria das árvores filogenéticas agrupou com precisão as espécies de morcegos, exceto para o promotor de LRP1B. Promotores de vários GSTs nas linhagens de morcegos Myotis e Rhinolophus exibiram evolução acelerada. Notavelmente, a ausência de sítios de ligação de SOX4 nos promotores de NF1 em espécies de longa vida sugere um padrão evolutivo adaptativo que contribui para a resistência ao câncer.

Conclusão: Este estudo fornece evidências de evolução acelerada nas regiões promotoras de importantes GSTs em morcegos, destacando padrões de SLFT específicos de linhagem associados à longevidade extrema. Esses achados contribuem para o entendimento da evolução regulatória subjacente à resistência ao câncer em mamíferos de vida longa.

Abstract

Background: Cancer prevalence varies significantly among mammals, despite the shared risk of developing cancer. The Doll-Armitage multistage model suggests that larger and longer-lived organisms should have higher cancer risks due to increased cell divisions and mutation accumulation. However, Peto's Paradox highlights that interspecies cancer rates do not correlate with body mass or lifespan, indicating that larger, longer-lived species may have evolved superior tumor suppression mechanisms. Bats, with their exceptional longevity relative to body size and high metabolic rates, provide a unique opportunity to study these mechanisms. This study investigates the molecular evolution of tumor suppressor gene (TSG) promoter regions in bats, focusing on the evolution of transcription factor binding sites (TFBS) within these promoters and their evolutionary conservation or acceleration.

Results: We selected 12 TSGs frequently mutated in pan-cancer screenings and retrieved the 1500 bp upstream regions of these genes' transcription start sites. Phylogenetic trees were generated using IQ-TREE, and the evolutionary rates of promoter regions were analyzed with phyloFit and phylo-P tools. Enrichment analysis of TFBS was conducted using the Ciiider software. Most phylogenetic trees accurately grouped bat species, except for the LRP1B promoter. Promoters of several TSGs in Myotis and Rhinolophus bat lineages exhibited accelerated evolution. Notably, the absence of SOX4 binding sites in NF1 promoters of long-lived species suggests an adaptive evolutionary pattern contributing to cancer resistance.

Conclusion: This study provides evidence of accelerated evolution in the promoter regions of key TSGs in bats, highlighting lineage-specific TFBS patterns associated with extreme longevity. These findings contribute to our understanding of the regulatory evolution underlying cancer resistance in long-lived mammals.

Background

Our current most accepted theory, the Doll-Armitage multistage model of oncogenesis (1), states that cancer is a multistage process where, during the organism's lifetime, somatic cell lineages accumulate mutations from endogenous or exogenous mutational factors. While most mutations are harmless, some can hit oncogenes (OGs) or tumor suppressor genes (TSGs) that can eventually drive the initiation and progression of malignancy. Thus, because at every cell division, somatic cells carry a risk of acquiring new mutations, this theory predicts that organisms with larger body sizes and extended longevities will have an increased risk of developing cancer. Indeed, this theory applies when we compare organisms within the same species both for body size and age (3–5). However, it is known that mammals' interspecies cancer rates do not correlate with body mass or lifespan (2). This means that, while most, if not all, mammals are at some risk of developing cancer, there are marked differences in their cancer prevalence (2).This mismatch between theoretical prediction and observation was named Peto's Paradox (6). This paradox suggests that evolution may have selected more efficient mechanisms of tumor suppression for species with greater lifespan and body mass, compensating for the increased cancer risk.

In mammals, body mass, lifespan, and many other life-history traits are allometrically correlated. Then, identifying organisms with extreme lifespan requires size correction. One way of doing so is to calculate the ratio of the observed by the expected lifespan, i.e. the longevity quotient (LQ). By this metric, bats - order Chiropetra - have by far the most extreme longevity of all mammals. Interestingly, 18 of 19 mammalian species with lifespans longer than humans relative to their body size are bat species (7). That, coupled with the observed high metabolic rates and their extraordinary immunity, make bats a remarkable taxon to study the evolution of TSGs (8,9).

Significant progress has been made in understanding the evolutionary patterns of Chiroptera's cancer-related protein-coding genes, yet the evolution of their cis-regulatory regions remains less explored (8, 10). In this context, this study focused on the molecular evolution of TSGs promoter regions, defined here as the 1500 bp upstream from the transcription start site (TSS). Specifically, our study is particularly interested in the promoters evolution of extremely long-lived bat lineages. Our aim was to investigate the enrichment and configuration of transcription factor binding sites (TFBS) within these promoter sequences and to examine their rates of evolutionary conservation or acceleration.

Materials and methods

Data collection and preprocessing

To reproduce Adams and Wilkinson (11) estimations of extreme longevity in mammals, we obtained maximum longevity and body mass records from AnAge database (12) and calculated the LQ, that is, the ratio of the observed to predicted maximum longevity given the species body mass. This parameter is calculated by the least squares regression of non-flying placental mammals, i.e. $\log10(\text{longevity}) = 0.5609 + \log10(\text{body mass}) \times 0.1868$. Organisms with LQ > 4.2 were classified as extremely long-lived. Because maximum longevity is expected to be more precise as the sample size increases, we only included acceptable quality records with medium, large or huge sample sizes (Table 1).

Table 1: Species included in this study their respective longevity quotient (LQ).

Order	Family	Species	Common name	LQ
Chiroptera	Vespertilionidae	Myotis myotis	Mouse-eared bat	5.452136
Chiroptera	Vespertilionidae	Myotis daubentonii	Daubenton's bat	5.159915
Chiroptera	Rhinolophidae	Rhinolophus ferrumequinum	Greater horseshoe bat	4.671660
Chiroptera	Pteropodidae	Pteropus giganteus	Indian flying fox	3.229012
Chiroptera	Vespertilionidae	Eptesicus fuscus	Big brown bat	2.907253
Chiroptera	Phyllostomidae	Artibeus jamaicensis	Jamaican fruit-eating bat	2.622967
Chiroptera	Pteropodidae	Rousettus aegyptiacus	Egyptian rousette	2.554069
Chiroptera	Pteropodidae	Pteropus vampyrus	Large flying fox	1.621653
Chiroptera	Vespertilionidae	Pipistrellus kuhlii	Kuhl's pipistrelle	1.573372
Chiroptera	Phyllostomidae	Phyllostomus discolor	Pale spear-nosed bat	1.223093
Primates	Hominidae	Homo sapiens	Human	4.285204
Primates	Hylobatidae	Hylobates moloch	Silvery gibbon	2.419890
Primates	Lorisidae	Nycticebus coucang	Slow loris	1.994013
Primates	Cercopithecidae	Trachypithecus francoisi	Francois's leaf monkey	1.371228
Pilosa	Megalonychidae	Choloepus didactylus	Southern two-toed sloth	1.976412
Rodentia	Cricetidae	Peromyscus eremicus	Cactus mouse	1.114799
Rodentia	Dipodidae	Jaculus jaculus	Lesser Egyptian jerboa	0.949124
Carnivora	Ursidae	Ursus americanus	American black bear	1.003271
Carnivora	Felidae	Panthera pardus	Leopard	0.980907
Carnivora	Hyaenidae	Hyaena hyaena	Striped hyena	0.949238
Carnivora	Canidae	Vulpes lagopus	Arctic fox	0.906021
Carnivora	Mustelidae	Meles meles	European badger	0.871221
Carnivora	Felidae	Neofelis nebulosa	Clouded leopard	0.859779
Proboscidea	Elephantidae	Loxodonta africana	African bush elephant	1.009154
Erinaceomorpha	Erinaceidae	Erinaceus europaeus	Western European hedgehog	0.933737

We selected a list of 10 TSGs that were found to be most frequently mutated across each of two big pan-cancer screenings (13,14). The combined lists amounted for 12 TSGs in total (TP53, KMT2D, KMT2C, PTEN, ARID1A, FAT1, FAT4, APC, ATM, ATRX, LRP1B and NF1) (Table S1). These genes have high clinical significance, and it is reasonable to suggest they may have played a crucial role in the evolution of cancer resistance mechanisms, especially in organisms facing strong selective pressures for enhanced cancer defenses. We retrieved the 1500 bp upstream of the Transcription Start Site (TSS) for orthologous genes across all eutherians with all 12 orthologous genes successfully localized, as listed in the NCBI database. Only ungapped, full-length, and high-quality sequences were maintained. We limited our analysis to promoter sequences for which species LQ data were available. The final set of NCBI gene IDs included in this study is provided in the supplementary material (Table S3).

IQ-TREE phylogenetic reconstruction

We aligned the promoter sequences using MAFFT (15), selecting the L-INS-i option and setting the alignment scoring matrix to Kimura kappa 2 PAM200. Phylogenetic trees for each promoter alignment were then generated using the maximum likelihood method via the IQ-TREE Web Server portal (16), with 1,000 bootstrap replicated for confidence.

Regulatory regions analysis

To generate a phyloFit (17) substitution model for each promoter sequence alignment, we first sampled 1,000 equally plausible phylogenetic trees for all species used in this study from the posterior distribution available on the VertLife webtool (18,19), covering 5,911 species. A consensus tree was then created using the Dendropy Python toolbox (20). This tree enabled us to infer an evolutionary model with the phyloFit program, using the Reversive Evolutionary Model (REV). Subsequently, we employed the phylo-P(21) tool to estimate the molecular evolution rates and assess the evolutionary conservation or acceleration for each promoter using the Likelihood Ratio Test (LRT) model and the CONACC mode, which outputs both conservation and acceleration scores.

As Adams and Wilkinson (11) has shown, extreme longevity has evolved independently in Myotis and Rhinolophus lineages. Therefore, it is likely that their unrelated evolutionary trajectories would display different patterns of acceleration and conservation. To account for that, these lineages were separately analyzed using the phylo-P subtree mode. This mode partition the tree into the subtree beneath the lineage of interest (Myotis or Rhinolophus) and the complementary supertree (all other species in the tree), then it is estimated the conservation/acceleration in the subtree given the supertree.

Lastly, we used the Ciiider software (22) for scanning and enrichment analysis. During the scanning stage, potential transcription factor binding sites (TFBSs) were predicted in the promoter sequences for each species, using the JASPAR 2020 CORE non-redundant vertebrate matrices (23). In the enrichment stage, we identified TFBSs that were significantly over- or under-represented compared to a background list of sequences provided by the software. All analyses were conducted with default parameters.

Results

For most of the promoter phylogenetic trees generated by the IQ-TREE software, the expected grouping of bat species and other mammals were observed (see Figures S1-S11). However, the LRP1B promoter (Figure 1) was an exception as the sequences of Mouse-eared bat (*Myotis myotis*) and African bush elephant (*Loxodonta africana)* appeared more closely related to each other than to their respective clades.

Furthemore, the phylo-P analysis revealed that the subtree comprising Daubenton's bat (*Myotis daubentonii)* and Mouse-eared bat (*Myotis myotis)* is experiencing accelerated evolution in the promoters of LRP1B, APC, FAT1, KMT2D, NF1 and PTEN compared to other species. Additionally, evidence of acceleration in the promoters of APC, ARID1A, ATM, ATRX, FAT1, KMT2C, KMT2D and PTEN was also observed in the evolution of the Greater horseshoe bat (*Rhinolophus ferrumequinum)* subtree (Table 2).

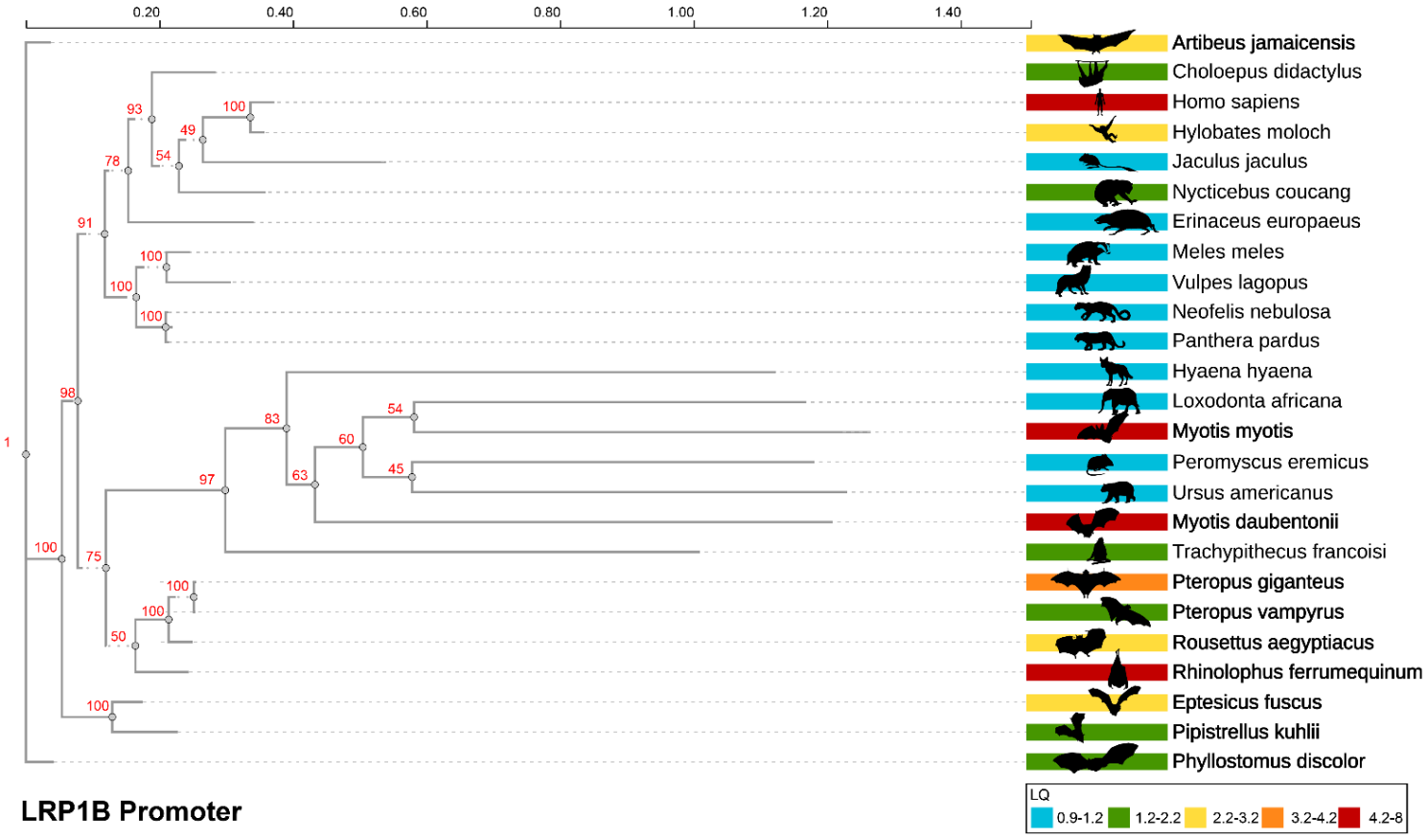

Figure 1: Unrooted maximum likelihood tree generated by IQ−TREE constructed from the promoter region of the LRP1B gene. Numbers above nodes represent bootstrap support and species color-coded with each respective longevity quotient.

Table 2: Phylo-P subtrees p-values (pval) for conservation or acceleration in all promoter sequences included in this study. Positive scores indicate evolutionary conservation, and negative scores (in bold) denote evolutionary acceleration.

	Myotis daubentonii - Myotis myotis promoter evolution.				
Feature	**null_scale**	**alt_scale**	**alt_subscale**	**lnlratio**	**pval**
APC_promoter	***0.98564***	***0.98524***	***1.02382***	***0.02132***	***-0.8364***
ARID1A_promoter	1.16325	1.16771	0.87614	0.37643	0.38557
ATM_promoter	0.95473	0.95484	0.99655	0.00053	0.97407
ATRX_promoter	0.97671	0.98655	0.59666	10.17503	0.00001
FAT1_promoter	***1.06555***	***1.04824***	***1.44148***	***8.06265***	***-0.00006***
FAT4_promoter	0.95614	0.95821	0.90168	0.22017	0.50696
KMT2C_promoter	1.16897	1.17389	0.83871	0.7821	0.21105
KMT2D_promoter	***1.10232***	***1.09973***	***1.40928***	***0.73184***	***-0.22634***
LRP1B_promoter	***0.99134***	***0.98998***	***1.01023***	***0.026***	***-0.81961***
NF1_promoter	***1.06512***	***1.06468***	***1.02098***	***0.01082***	***-0.88307***
PTEN_promoter	***1.02515***	***1.02118***	***1.10652***	***0.59199***	***-0.27655***
TP53_promoter	1.02345	1.02385	0.98313	0.00871	0.89499

	Rhinolophus ferrumequinum promoter evolution.				
Feature	**null_scale**	**alt_scale**	**alt_subscale**	**lnlratio**	**pval**
APC_promoter	***0.98564***	***0.98496***	***1.02993***	***0.04677***	***-0.75973***
ARID1A_promoter	***1.16325***	***1.15835***	***1.16718***	***0.52571***	***-0.30518***
ATM_promoter	***0.95473***	***0.9544***	***1.01615***	***0.0081***	***-0.89871***
ATRX_promoter	***0.97671***	***0.97615***	***1.02916***	***0.02968***	***-0.8075***
FAT1_promoter	***1.06555***	***1.06336***	***1.11192***	***0.27572***	***-0.45773***
FAT4_promoter	0.95614	0.95806	0.90484	0.2031	0.52391
KMT2C_promoter	***1.16897***	***1.16529***	***1.13858***	***0.42536***	***-0.35635***
KMT2D_promoter	***1.10232***	***1.09644***	***1.34609***	***1.53002***	***-0.08024***
LRP1B_promoter	0.99134	0.99247	0.94879	0.11822	0.6268
NF1_promoter	***1.06512***	***1.06101***	***1.09254***	***0.49237***	***-0.32103***
PTEN_promoter	1.02515	1.02561	0.98339	0.01062	0.88412
TP53_promoter	1.02345	1.02395	0.97598	0.01523	0.86145

For the Ciiider analysis, no TFBSs distribution and enrichment pattern could be detected that were common for all extremely long-lived bats and clearly distinguishes them from other mammals in the promoters of TP53, KMT2D, KMT2C, PTEN, ARID1A, FAT1, FAT4, APC, ATM and ATRX (Figures S12-S22). However, in the NF1 promoter, we identified a consistent pattern of very similar TFBSs distribution among organisms known for extreme longevity. Notably, none of them had a SOX4 bidding site motif (Figure 2). Conversely, in the case of the LRP1B promoter sequences for Mouse-eared bat (*Myotis myotis*) and African bush elephant

(*Loxodonta africana),* we were unable to detect a TFBS pattern that could explain their clustering (Figure 3).

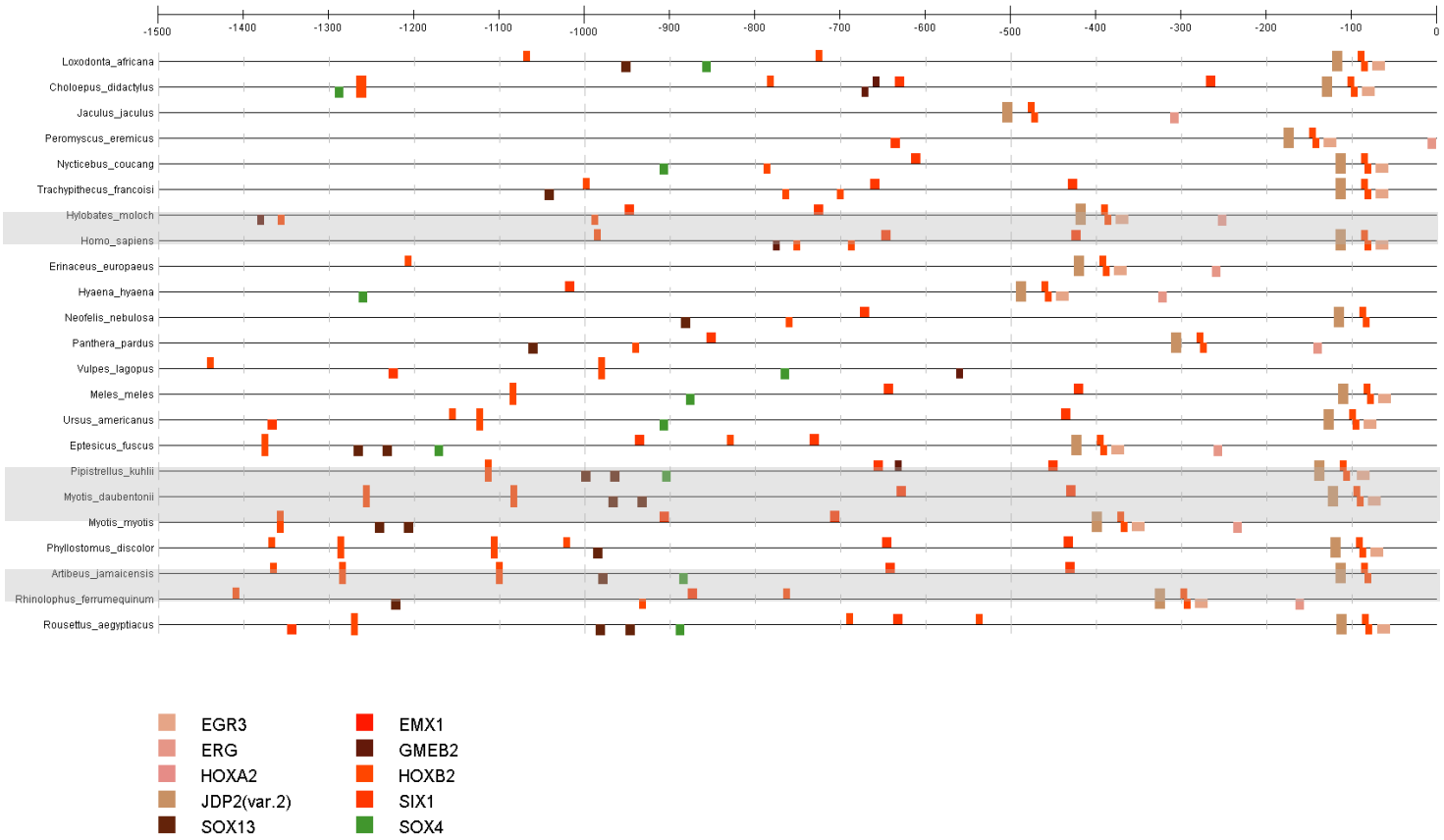

Figure 2: Ciiider enriched predictions of transcription factors binding sites in NF1 promoters' sequences. Species with LQ>4.2 are highlighted.

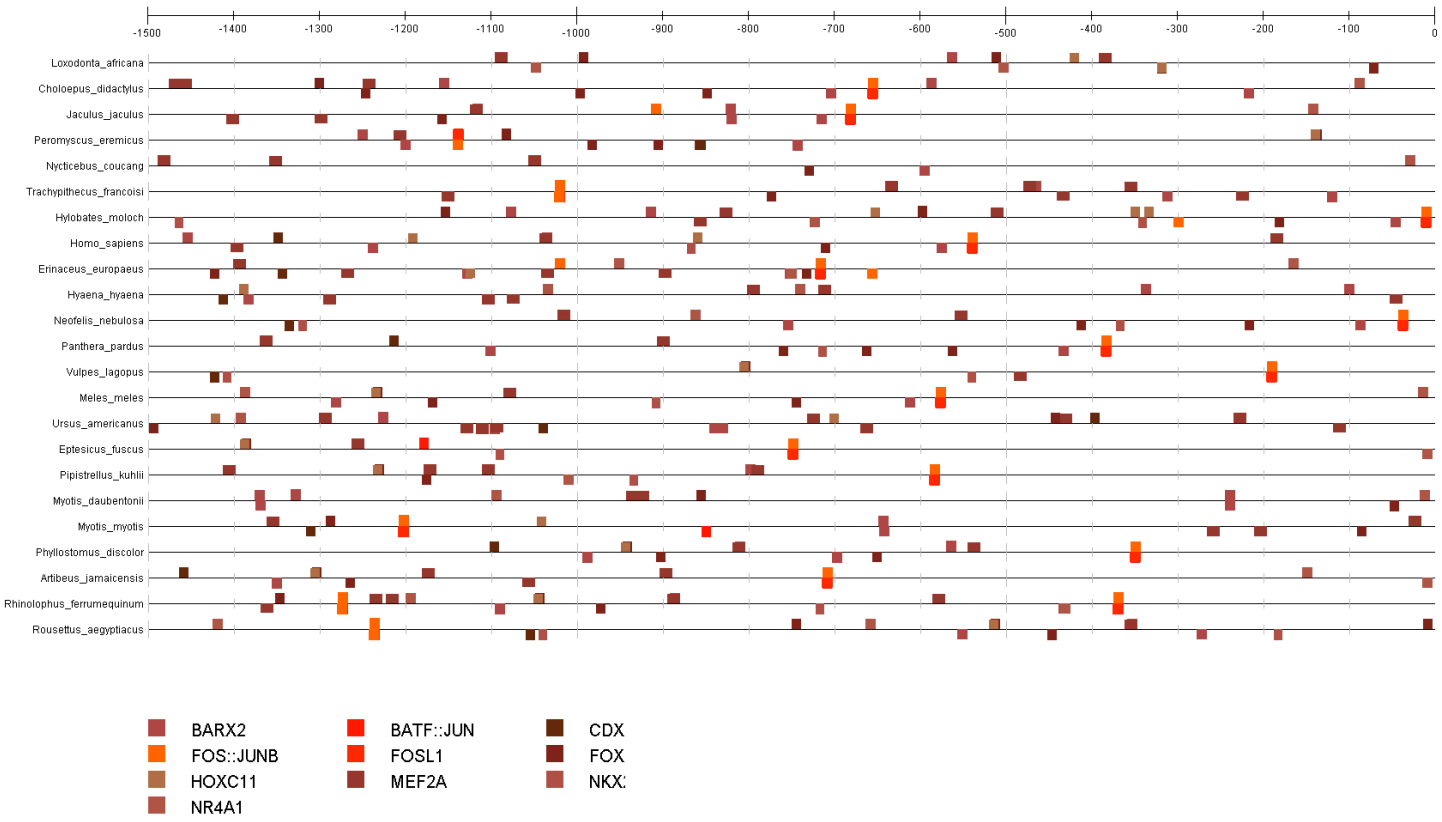

Figure 3: Ciiider enriched predictions of transcription factors binding sites in LRP1B promoters' sequences. Highly complex and variable distribution of TFBSs.

Discussion

In this study we explored the molecular evolution of TSGs promoters in bats, focusing on their evolutionary dynamics and the distribution and enrichment patterns of TFBSs within these regions. Our results revealed accelerated evolution in the promoter regions of several key TSGs in the Myotis and Rhinolophus bat lineages, which are known for their extreme longevity. Additionally, we identified a distinct absence of SOX4 binding sites in the *NF1* promoter among species with extreme longevity, suggesting a possible adaptive mechanism contributing to cancer resistance. These lineage-specific patterns in TFBS enrichment provide important insights into the regulatory evolution associated with cancer resistance in long-lived mammals.

Aligning non-coding regions is notably challenging due to their neutrally evolving nature and fewer constraints. Nevertheless, we were able to accurately capture the most accepted species tree topology for most promoters. However, in the case of the LRP1B promoter, African bush elephant (*Loxodonta africana)* and Mouse-eared bat (*Myotis myotis*) clustered together in an unexpected node. Such phylogenetic mismatches between gene trees and the more

comprehensive species tree are fairly common in nature and can be explained by phenomena such as molecular convergence due to similar mutation biases or adaptive convergence (24,25). Although African bush elephant (*Loxodonta africana)* does not have a particularly high LQ, elephants are known to be particularly resistant to cancer (26). This supports the hypothesis of evolutionary convergence or rapid evolution of regulatory elements for this promoter. However, the absence of a clear signal from the enrichment analysis reduces the likelihood of convergence in TFBSs patterns.

An intriguing outcome of our analysis is the absence of the SOX4 binding site in the NF1 promoter sequences of organisms exhibiting extreme longevity. This finding is notable because SOX4 is a pioneer transcription factor associated with mammary oncogenesis and tumor progression, known to inhibit cell differentiation and sustain stemness in colorectal cancer cells. This pattern may represent an adaptive mechanism, potentially explaining the accelerated evolution of this promoter in both studied lineages (27, 28).

Additionally, our phylo-P analysis identified promoters undergoing lineage-specific accelerated evolution, suggesting avenues for further comparative studies. Notably, the promoters of genes LRP1B and PTEN were found to be undergoing accelerated evolution in Myotis but not in Rhinolophus. Conversely, the promoters of ARID1A, ATM, ATRX and KMT2C were found to be undergoing accelerated evolution in Rhinolophus but not in Myotis. Suggesting that these lineages have evolved distinct regulatory mechanisms for these lineages under similar selection pressures. Yet, more sensitive analyses and experimental validations are needed to correlate these genetic predictions with phenotypic observations.

Conclusion

In this study, we analyzed the evolution of regulatory regions for 12 tumor suppressor genes (TSGs) in bats. We found evidence of evolutionary acceleration in the promoter of genes APC, ARID1A, ATM, ATRX, FAT1, KMT2C, KMT2D, LRP1B, NF1, and PTEN. Additionally, we identified lineage-specific TFBSs enrichment patterns likely associated with extreme longevity. In conclusion, our study provides a valuable overview of the regulatory landscape that may influence cancer resistance evolution.

Data Availability

All the data and methods used to provide support to our analysis are contained within the manuscript and in the supplementary materials.

References

1.Armitage P, Doll R. The Age Distribution of Cancer and a Multi-stage Theory of Carcinogenesis. Br J Cancer. 1954 Mar 1;8(1):1–12.

2. Vincze O, Colchero F, Lemaître JF, Conde DA, Pavard S, Bieuville M, et al. Cancer risk across mammals. Nature. 2021;(April).

3. Wirén S, Häggström C, Ulmer H, Manjer J, Bjørge T, Nagel G, et al. Pooled cohort study on height and risk of cancer and cancer death. Cancer Causes Control CCC. 2014 Feb;25(2):151–9.

4. Nunney L. Size matters: height, cell number and a person's risk of cancer. Proc Biol Sci. 2018 Oct 24;285(1889):20181743.

5. Fleming JM, Creevy KE, Promislow DEL. Mortality in north american dogs from 1984 to 2004: an investigation into age-, size-, and breed-related causes of death. J Vet Intern Med. 2011;25(2):187–98.

6. Peto R, Roe FJ, Lee PN, Levy L, Clack J. Cancer and ageing in mice and men. Br J Cancer. 1975 Oct;32(4):411–26.

7. Foley NM, Hughes GM, Huang Z, Clarke M, Jebb D, Whelan CV, et al. Growing old, yet staying young: The role of telomeres in bats' exceptional longevity. Sci Adv. 4(2):eaao0926.

8. Moreno Santillán DD, Lama TM, Gutierrez Guerrero YT, Brown AM, Donat P, Zhao H, et al. Large‐scale genome sampling reveals unique immunity and metabolic adaptations in bats. Mol Ecol. 2021 Dec;30(23):6449–67.

9. Munshi-South J, Wilkinson GS. Bats and birds: Exceptional longevity despite high metabolic rates. Ageing Res Rev. 2010 Jan;9(1):12–9.

10.MacDonald N, Raven N, Diep W, Evans S, Pannipitiya S, Bramwell G, et al. The molecular evolution of cancer associated genes in mammals. Sci Rep. 2024 May 22;14(1):11650.

11.Wilkinson GS, Adams DM. Recurrent evolution of extreme longevity in bats. Biol Lett. 2019 Apr;15(4):20180860.

12.Tacutu R, Thornton D, Johnson E, Budovsky A, Barardo D, Craig T, et al. Human Ageing Genomic Resources: new and updated databases. Nucleic Acids Res. 2018 Jan 4;46(D1):D1083–90.

13.Mendiratta G, Mendiratta G, Mendiratta G, Ke E, Ke E, Aziz M, et al. Cancer gene mutation frequencies for the U.S. population. Nat Commun. 2021;

14. Sondka Z, Bamford S, Cole CG, Ward SA, Dunham I, Forbes SA. The COSMIC Cancer Gene Census: describing genetic dysfunction across all human cancers. Nat Rev Cancer. 2018;18(11):696–705.

15. Katoh K, Standley DM. MAFFT Multiple Sequence Alignment Software Version 7: Improvements in Performance and Usability. Mol Biol Evol. 2013 Apr 1;30(4):772–80.

16. Nguyen LT, Schmidt HA, von Haeseler A, Minh BQ. IQ-TREE: a fast and effective stochastic algorithm for estimating maximum-likelihood phylogenies. Mol Biol Evol. 2015 Jan;32(1):268–74.

17. Siepel A, Haussler D. Phylogenetic estimation of context-dependent substitution rates by maximum likelihood. Mol Biol Evol. 2004 Mar;21(3):468–88.

18. Upham NS, Esselstyn JA, Jetz W. Inferring the mammal tree: Species-level sets of phylogenies for questions in ecology, evolution, and conservation. PLOS Biol. 2019 de dez. de;17(12):e3000494.

19. Upham NS, Esselstyn JA, Jetz W. Ecological causes of uneven mammal diversity [Internet]. bioRxiv; 2023 [cited 2024 Jul 30]. p. 504803. Available from: https://www.biorxiv.org/content/10.1101/504803v5

20. Moreno MA, Holder MT, Sukumaran J. DendroPy 5: a mature Python library for phylogenetic computing [Internet]. arXiv; 2024 [cited 2024 Jul 30]. Available from: http://arxiv.org/abs/2405.14120

21. Pollard KS, Hubisz MJ, Rosenbloom KR, Siepel A. Detection of nonneutral substitution rates on mammalian phylogenies. Genome Res. 2010 Jan 1;20(1):110–21.

22. Gearing LJ, Cumming HE, Chapman R, Finkel AM, Woodhouse IB, Luu K, et al. CiiiDER: A tool for predicting and analysing transcription factor binding sites. PLOS ONE. 2019 de set de;14(9):e0215495.

23. Fornes O, Castro-Mondragon JA, Khan A, van der Lee R, Zhang X, Richmond PA, et al. JASPAR 2020: update of the open-access database of transcription factor binding profiles. Nucleic Acids Res. 2020 Jan 8;48(D1):D87–92.

24. Hao Y, Qu Y, Song G, Lei F. Genomic Insights into the Adaptive Convergent Evolution. Curr Genomics. 2019 Feb;20(2):81–9.

25. Arbuckle K, Speed MP. Analysing Convergent Evolution: A Practical Guide to Methods. In: Pontarotti P, editor. Evolutionary Biology [Internet]. Cham: Springer International Publishing; 2016 [cited 2024 Apr 15]. p. 23–36. Available from: http://link.springer.com/10.1007/978-3-319-41324-2_2

26.Seluanov A, Gladyshev VN, Vijg J, Gorbunova V. Mechanisms of cancer resistance in long-lived mammals. Nat Rev Cancer. 2018;18(7):433–41.

27.Roukens MG, Frederiks CL, Seinstra D, Braccioli L, Khalil AA, Pals C, et al. Regulation of a progenitor gene program by SOX4 is essential for mammary tumor proliferation. Oncogene. 2021 Nov;40(45):6343–53.

28.Liu J, Qiu J, Zhang Z, Zhou L, Li Y, Ding D, et al. SOX4 maintains the stemness of cancer cells via transcriptionally enhancing HDAC1 revealed by comparative proteomics study. Cell Biosci. 2021 Jan 22;11(1):23.

SUPPLEMENTARY MATERIALS

Molecular Evolution of Tumor Suppressor Gene Promoters in Bats: Unraveling Peto's Paradox with Phylogenetic and TFBS Enrichment Studies

Chaves, Mathias Rennó[1]; Nery, Mariana Freitas[2]*.

[1] Dept. of Chemical and Biological Sciences, Institute of Biosciences of Botucatu, São Paulo State University, Distrito de Rubião Júnior, Rua Prof. Dr. Antonio Celso Wagner Zanin, 250 Botucatu/SP 18618-689

[2] Dept of Genetics, Evolution, Microbiology & Immunology, Institute of Biology, University of Campinas, Rua Monteiro Lobato, 255 Campinas/SP 13083-862

* marinery@unicamp.br; Tel.: + 55 21 3938-735

Table S1: List of most frequently mutated genes and its reported frequencies.

Gene Symbol	10 most frequently mutated genes (Mendiratta G, 2021)	10 most frequently mutated genes (Sondka Z, 2022)
APC	5.87%	10.09%
ARID1A	6.69%	6.96%
ATM	4.12%	5.49%
ATRX	5.69%	
FAT1	6.22%	6.64%
FAT4		9.46%
KMT2C	8.11%	9.13%
KMT2D	8.33%	9.17%
LRP1B		13.08%
NF1	5.29%	
PTEN	7.47%	5.97%
TP53	37.53%	34.54%

Table S2: Species used in this study and the respective accession numbers from NCBI.

Gene_symbol	taxon_ID	Order	Family	Species	NCBI_gene_ID
APC	494514	Carnivora	Canidae	Vulpes lagopus	121489860
	61452	Carnivora	Felidae	Neofelis nebulosa	131509338
	9691	Carnivora	Felidae	Panthera pardus	109267599
	95912	Carnivora	Hyaenidae	Hyaena hyaena	120236758
	9662	Carnivora	Mustelidae	Meles meles	123938259
	9643	Carnivora	Ursidae	Ursus americanus	123779308
	9417	Chiroptera	Phyllostomidae	Artibeus jamaicensis	119065104
	89673	Chiroptera	Phyllostomidae	Phyllostomus discolor	114493533
	143291	Chiroptera	Pteropodidae	Pteropus giganteus	120590819
	132908	Chiroptera	Pteropodidae	Pteropus vampyrus	105295478
	9407	Chiroptera	Pteropodidae	Rousettus aegyptiacus	107512008
	59479	Chiroptera	Rhinolophidae	Rhinolophus ferrumequinum	117024772

	29078	Chiroptera	Vespertilionidae	Eptesicus fuscus	103288721
	98922	Chiroptera	Vespertilionidae	Myotis daubentonii	132233350
	51298	Chiroptera	Vespertilionidae	Myotis myotis	118655759
	59472	Chiroptera	Vespertilionidae	Pipistrellus kuhlii	118703090
	9365	Erinaceomorpha	Erinaceidae	Erinaceus europaeus	103125270
	27675	Pilosa	Megalonychidae	Choloepus didactylus	119508575
	54180	Primates	Cercopithecidae	Trachypithecus francoisi	117064818
	9606	Primates	Hominidae	Homo sapiens	324
	81572	Primates	Hylobatidae	Hylobates moloch	116470936
	9470	Primates	Lorisidae	Nycticebus coucang	128568996
	9785	Proboscidea	Elephantidae	Loxodonta africana	100659017
	42410	Rodentia	Cricetidae	Peromyscus eremicus	131895971
	51337	Rodentia	Dipodidae	Jaculus jaculus	101616891
ARID1A	494514	Carnivora	Canidae	Vulpes lagopus	121496698
	61452	Carnivora	Felidae	Neofelis nebulosa	131505208
	9691	Carnivora	Felidae	Panthera pardus	109256756
	95912	Carnivora	Hyaenidae	Hyaena hyaena	120231175
	9662	Carnivora	Mustelidae	Meles meles	123936659
	9643	Carnivora	Ursidae	Ursus americanus	123782467
	9417	Chiroptera	Phyllostomidae	Artibeus jamaicensis	119042231
	89673	Chiroptera	Phyllostomidae	Phyllostomus discolor	114497988
	143291	Chiroptera	Pteropodidae	Pteropus giganteus	120596166
	132908	Chiroptera	Pteropodidae	Pteropus vampyrus	105290496
	9407	Chiroptera	Pteropodidae	Rousettus aegyptiacus	107503535
	59479	Chiroptera	Rhinolophidae	Rhinolophus ferrumequinum	117026650
	29078	Chiroptera	Vespertilionidae	Eptesicus fuscus	103291912
	98922	Chiroptera	Vespertilionidae	Myotis daubentonii	132231487
	51298	Chiroptera	Vespertilionidae	Myotis myotis	118675026
	59472	Chiroptera	Vespertilionidae	Pipistrellus kuhlii	118722766
	9365	Erinaceomorpha	Erinaceidae	Erinaceus europaeus	103121943
	27675	Pilosa	Megalonychidae	Choloepus didactylus	119527725
	54180	Primates	Cercopithecidae	Trachypithecus francoisi	117093056
	9606	Primates	Hominidae	Homo sapiens	8289
	81572	Primates	Hylobatidae	Hylobates moloch	116813128
	9470	Primates	Lorisidae	Nycticebus coucang	128575386
	9785	Proboscidea	Elephantidae	Loxodonta africana	100673206
	42410	Rodentia	Cricetidae	Peromyscus eremicus	131904154
	51337	Rodentia	Dipodidae	Jaculus jaculus	101617287
ATM	494514	Carnivora	Canidae	Vulpes lagopus	121500044
	61452	Carnivora	Felidae	Neofelis nebulosa	131486766
	9691	Carnivora	Felidae	Panthera pardus	109278700
	95912	Carnivora	Hyaenidae	Hyaena hyaena	120229863
	9662	Carnivora	Mustelidae	Meles meles	123949760
	9643	Carnivora	Ursidae	Ursus americanus	123792533
	9417	Chiroptera	Phyllostomidae	Artibeus jamaicensis	119059255

	89673	Chiroptera	Phyllostomidae	Phyllostomus discolor	114498399
	143291	Chiroptera	Pteropodidae	Pteropus giganteus	120619030
	132908	Chiroptera	Pteropodidae	Pteropus vampyrus	105297463
	9407	Chiroptera	Pteropodidae	Rousettus aegyptiacus	107518682
	59479	Chiroptera	Rhinolophidae	Rhinolophus ferrumequinum	117030407
	29078	Chiroptera	Vespertilionidae	Eptesicus fuscus	103299223
	98922	Chiroptera	Vespertilionidae	Myotis daubentonii	132240592
	51298	Chiroptera	Vespertilionidae	Myotis myotis	118664416
	59472	Chiroptera	Vespertilionidae	Pipistrellus kuhlii	118712974
	9365	Erinaceomorpha	Erinaceidae	Erinaceus europaeus	103128879
	27675	Pilosa	Megalonychidae	Choloepus didactylus	119538409
	54180	Primates	Cercopithecidae	Trachypithecus francoisi	117081112
	9606	Primates	Hominidae	Homo sapiens	472
	81572	Primates	Hylobatidae	Hylobates moloch	116476898
	9470	Primates	Lorisidae	Nycticebus coucang	128587595
	9785	Proboscidea	Elephantidae	Loxodonta africana	100663914
	42410	Rodentia	Cricetidae	Peromyscus eremicus	131915004
	51337	Rodentia	Dipodidae	Jaculus jaculus	101615318
ATRX	494514	Carnivora	Canidae	Vulpes lagopus	121482748
	61452	Carnivora	Felidae	Neofelis nebulosa	131501994
	9691	Carnivora	Felidae	Panthera pardus	109258948
	95912	Carnivora	Hyaenidae	Hyaena hyaena	120224489
	9662	Carnivora	Mustelidae	Meles meles	123934546
	9643	Carnivora	Ursidae	Ursus americanus	123794872
	9417	Chiroptera	Phyllostomidae	Artibeus jamaicensis	119039451
	89673	Chiroptera	Phyllostomidae	Phyllostomus discolor	114505456
	143291	Chiroptera	Pteropodidae	Pteropus giganteus	120591613
	132908	Chiroptera	Pteropodidae	Pteropus vampyrus	105308888
	9407	Chiroptera	Pteropodidae	Rousettus aegyptiacus	107502455
	59479	Chiroptera	Rhinolophidae	Rhinolophus ferrumequinum	117021243
	29078	Chiroptera	Vespertilionidae	Eptesicus fuscus	103303647
	98922	Chiroptera	Vespertilionidae	Myotis daubentonii	132224260
	51298	Chiroptera	Vespertilionidae	Myotis myotis	118654707
	59472	Chiroptera	Vespertilionidae	Pipistrellus kuhlii	118719981
	9365	Erinaceomorpha	Erinaceidae	Erinaceus europaeus	103123688
	27675	Pilosa	Megalonychidae	Choloepus didactylus	119524085
	54180	Primates	Cercopithecidae	Trachypithecus francoisi	117078248
	9606	Primates	Hominidae	Homo sapiens	546
	81572	Primates	Hylobatidae	Hylobates moloch	116811105
	9470	Primates	Lorisidae	Nycticebus coucang	128577216
	9785	Proboscidea	Elephantidae	Loxodonta africana	100657543
	42410	Rodentia	Cricetidae	Peromyscus eremicus	131899963
	51337	Rodentia	Dipodidae	Jaculus jaculus	101611330
FAT1	494514	Carnivora	Canidae	Vulpes lagopus	121490156
	61452	Carnivora	Felidae	Neofelis nebulosa	131506426

	9691	Carnivora	Felidae	Panthera pardus	109250986
	95912	Carnivora	Hyaenidae	Hyaena hyaena	120237780
	9662	Carnivora	Mustelidae	Meles meles	123937257
	9643	Carnivora	Ursidae	Ursus americanus	123784490
	9417	Chiroptera	Phyllostomidae	Artibeus jamaicensis	119036811
	89673	Chiroptera	Phyllostomidae	Phyllostomus discolor	114508524
	143291	Chiroptera	Pteropodidae	Pteropus giganteus	120583814
	132908	Chiroptera	Pteropodidae	Pteropus vampyrus	105294725
	9407	Chiroptera	Pteropodidae	Rousettus aegyptiacus	107510432
	59479	Chiroptera	Rhinolophidae	Rhinolophus ferrumequinum	117021721
	29078	Chiroptera	Vespertilionidae	Eptesicus fuscus	103290317
	98922	Chiroptera	Vespertilionidae	Myotis daubentonii	132228715
	51298	Chiroptera	Vespertilionidae	Myotis myotis	118651730
	59472	Chiroptera	Vespertilionidae	Pipistrellus kuhlii	118730783
	9365	Erinaceomorpha	Erinaceidae	Erinaceus europaeus	103108711
	27675	Pilosa	Megalonychidae	Choloepus didactylus	119530082
	54180	Primates	Cercopithecidae	Trachypithecus francoisi	117086231
	9606	Primates	Hominidae	Homo sapiens	2195
	81572	Primates	Hylobatidae	Hylobates moloch	116466091
	9470	Primates	Lorisidae	Nycticebus coucang	128581363
	9785	Proboscidea	Elephantidae	Loxodonta africana	100660201
	42410	Rodentia	Cricetidae	Peromyscus eremicus	131894760
	51337	Rodentia	Dipodidae	Jaculus jaculus	101608925
FAT4	494514	Carnivora	Canidae	Vulpes lagopus	121493056
	61452	Carnivora	Felidae	Neofelis nebulosa	131507098
	9691	Carnivora	Felidae	Panthera pardus	109249030
	95912	Carnivora	Hyaenidae	Hyaena hyaena	120245820
	9662	Carnivora	Mustelidae	Meles meles	123936637
	9643	Carnivora	Ursidae	Ursus americanus	123793300
	9417	Chiroptera	Phyllostomidae	Artibeus jamaicensis	119037606
	89673	Chiroptera	Phyllostomidae	Phyllostomus discolor	114504002
	143291	Chiroptera	Pteropodidae	Pteropus giganteus	120616238
	132908	Chiroptera	Pteropodidae	Pteropus vampyrus	105302714
	9407	Chiroptera	Pteropodidae	Rousettus aegyptiacus	107518502
	59479	Chiroptera	Rhinolophidae	Rhinolophus ferrumequinum	117037601
	29078	Chiroptera	Vespertilionidae	Eptesicus fuscus	103287635
	98922	Chiroptera	Vespertilionidae	Myotis daubentonii	132235548
	51298	Chiroptera	Vespertilionidae	Myotis myotis	118658370
	59472	Chiroptera	Vespertilionidae	Pipistrellus kuhlii	118710942
	9365	Erinaceomorpha	Erinaceidae	Erinaceus europaeus	103125555
	27675	Pilosa	Megalonychidae	Choloepus didactylus	119529840
	54180	Primates	Cercopithecidae	Trachypithecus francoisi	117085886
	9606	Primates	Hominidae	Homo sapiens	79633
	81572	Primates	Hylobatidae	Hylobates moloch	116463664
	9470	Primates	Lorisidae	Nycticebus coucang	128575791

	9785	Proboscidea	Elephantidae	Loxodonta africana	100673183
	42410	Rodentia	Cricetidae	Peromyscus eremicus	131912821
	51337	Rodentia	Dipodidae	Jaculus jaculus	101603917
KMT2C	494514	Carnivora	Canidae	Vulpes lagopus	121489565
	61452	Carnivora	Felidae	Neofelis nebulosa	131508698
	9691	Carnivora	Felidae	Panthera pardus	109252401
	95912	Carnivora	Hyaenidae	Hyaena hyaena	120230926
	9662	Carnivora	Mustelidae	Meles meles	123951644
	9643	Carnivora	Ursidae	Ursus americanus	123788754
	9417	Chiroptera	Phyllostomidae	Artibeus jamaicensis	119039227
	89673	Chiroptera	Phyllostomidae	Phyllostomus discolor	114507487
	143291	Chiroptera	Pteropodidae	Pteropus giganteus	120601517
	132908	Chiroptera	Pteropodidae	Pteropus vampyrus	105303780
	9407	Chiroptera	Pteropodidae	Rousettus aegyptiacus	107520298
	59479	Chiroptera	Rhinolophidae	Rhinolophus ferrumequinum	117018143
	29078	Chiroptera	Vespertilionidae	Eptesicus fuscus	103301773
	98922	Chiroptera	Vespertilionidae	Myotis daubentonii	132242596
	51298	Chiroptera	Vespertilionidae	Myotis myotis	118679443
	59472	Chiroptera	Vespertilionidae	Pipistrellus kuhlii	118704757
	9365	Erinaceomorpha	Erinaceidae	Erinaceus europaeus	103124932
	27675	Pilosa	Megalonychidae	Choloepus didactylus	119533887
	54180	Primates	Cercopithecidae	Trachypithecus francoisi	117072766
	9606	Primates	Hominidae	Homo sapiens	58508
	81572	Primates	Hylobatidae	Hylobates moloch	116814558
	9470	Primates	Lorisidae	Nycticebus coucang	128598165
	9785	Proboscidea	Elephantidae	Loxodonta africana	100673765
	42410	Rodentia	Cricetidae	Peromyscus eremicus	131906906
	51337	Rodentia	Dipodidae	Jaculus jaculus	101614453
KMT2D	494514	Carnivora	Canidae	Vulpes lagopus	121480058
	61452	Carnivora	Felidae	Neofelis nebulosa	131519658
	9691	Carnivora	Felidae	Panthera pardus	109249058
	95912	Carnivora	Hyaenidae	Hyaena hyaena	120223002
	9662	Carnivora	Mustelidae	Meles meles	123946011
	9643	Carnivora	Ursidae	Ursus americanus	123794786
	9417	Chiroptera	Phyllostomidae	Artibeus jamaicensis	119042258
	89673	Chiroptera	Phyllostomidae	Phyllostomus discolor	114512768
	143291	Chiroptera	Pteropodidae	Pteropus giganteus	120618206
	132908	Chiroptera	Pteropodidae	Pteropus vampyrus	105297532
	9407	Chiroptera	Pteropodidae	Rousettus aegyptiacus	107514237
	59479	Chiroptera	Rhinolophidae	Rhinolophus ferrumequinum	117028056
	29078	Chiroptera	Vespertilionidae	Eptesicus fuscus	129149802
	98922	Chiroptera	Vespertilionidae	Myotis daubentonii	132227534
	51298	Chiroptera	Vespertilionidae	Myotis myotis	118650974
	59472	Chiroptera	Vespertilionidae	Pipistrellus kuhlii	118730318
	9365	Erinaceomorpha	Erinaceidae	Erinaceus europaeus	103118302

	27675	Pilosa	Megalonychidae	Choloepus didactylus	119541268
	54180	Primates	Cercopithecidae	Trachypithecus francoisi	117090180
	9606	Primates	Hominidae	Homo sapiens	8085
	81572	Primates	Hylobatidae	Hylobates moloch	116461666
	9470	Primates	Lorisidae	Nycticebus coucang	128560725
	9785	Proboscidea	Elephantidae	Loxodonta africana	100670013
	42410	Rodentia	Cricetidae	Peromyscus eremicus	131897101
	51337	Rodentia	Dipodidae	Jaculus jaculus	101616783
LRP1B	494514	Carnivora	Canidae	Vulpes lagopus	121482090
	61452	Carnivora	Felidae	Neofelis nebulosa	131503750
	9691	Carnivora	Felidae	Panthera pardus	109270483
	95912	Carnivora	Hyaenidae	Hyaena hyaena	120224255
	9662	Carnivora	Mustelidae	Meles meles	123950960
	9643	Carnivora	Ursidae	Ursus americanus	123782859
	9417	Chiroptera	Phyllostomidae	Artibeus jamaicensis	119064070
	89673	Chiroptera	Phyllostomidae	Phyllostomus discolor	114494331
	143291	Chiroptera	Pteropodidae	Pteropus giganteus	120596804
	132908	Chiroptera	Pteropodidae	Pteropus vampyrus	105288362
	9407	Chiroptera	Pteropodidae	Rousettus aegyptiacus	107505929
	59479	Chiroptera	Rhinolophidae	Rhinolophus ferrumequinum	117026234
	29078	Chiroptera	Vespertilionidae	Eptesicus fuscus	103287815
	98922	Chiroptera	Vespertilionidae	Myotis daubentonii	132238872
	51298	Chiroptera	Vespertilionidae	Myotis myotis	118662069
	59472	Chiroptera	Vespertilionidae	Pipistrellus kuhlii	118709434
	9365	Erinaceomorpha	Erinaceidae	Erinaceus europaeus	103128755
	27675	Pilosa	Megalonychidae	Choloepus didactylus	119544115
	54180	Primates	Cercopithecidae	Trachypithecus francoisi	117094219
	9606	Primates	Hominidae	Homo sapiens	53353
	81572	Primates	Hylobatidae	Hylobates moloch	116462987
	9470	Primates	Lorisidae	Nycticebus coucang	128590115
	9785	Proboscidea	Elephantidae	Loxodonta africana	100673742
	42410	Rodentia	Cricetidae	Peromyscus eremicus	131907712
	51337	Rodentia	Dipodidae	Jaculus jaculus	101604992
NF1	494514	Carnivora	Canidae	Vulpes lagopus	121474134
	61452	Carnivora	Felidae	Neofelis nebulosa	131497502
	9691	Carnivora	Felidae	Panthera pardus	109251797
	95912	Carnivora	Hyaenidae	Hyaena hyaena	120245671
	9662	Carnivora	Mustelidae	Meles meles	123929785
	9643	Carnivora	Ursidae	Ursus americanus	123776860
	9417	Chiroptera	Phyllostomidae	Artibeus jamaicensis	119050476
	89673	Chiroptera	Phyllostomidae	Phyllostomus discolor	114502466
	143291	Chiroptera	Pteropodidae	Pteropus giganteus	120620932
	132908	Chiroptera	Pteropodidae	Pteropus vampyrus	105291944
	9407	Chiroptera	Pteropodidae	Rousettus aegyptiacus	107497399
	59479	Chiroptera	Rhinolophidae	Rhinolophus ferrumequinum	117013151

	29078	Chiroptera	Vespertilionidae	Eptesicus fuscus	103291696
	98922	Chiroptera	Vespertilionidae	Myotis daubentonii	132218330
	51298	Chiroptera	Vespertilionidae	Myotis myotis	118671796
	59472	Chiroptera	Vespertilionidae	Pipistrellus kuhlii	118728122
	9365	Erinaceomorpha	Erinaceidae	Erinaceus europaeus	103120400
	27675	Pilosa	Megalonychidae	Choloepus didactylus	119514194
	54180	Primates	Cercopithecidae	Trachypithecus francoisi	117067564
	9606	Primates	Hominidae	Homo sapiens	4763
	81572	Primates	Hylobatidae	Hylobates moloch	116474531
	9470	Primates	Lorisidae	Nycticebus coucang	128569537
	9785	Proboscidea	Elephantidae	Loxodonta africana	100664100
	42410	Rodentia	Cricetidae	Peromyscus eremicus	131917470
	51337	Rodentia	Dipodidae	Jaculus jaculus	101607960
PTEN	494514	Carnivora	Canidae	Vulpes lagopus	121475822
	61452	Carnivora	Felidae	Neofelis nebulosa	131492612
	9691	Carnivora	Felidae	Panthera pardus	109255395
	95912	Carnivora	Hyaenidae	Hyaena hyaena	120235953
	9662	Carnivora	Mustelidae	Meles meles	123954853
	9643	Carnivora	Ursidae	Ursus americanus	123795550
	9417	Chiroptera	Phyllostomidae	Artibeus jamaicensis	119057730
	89673	Chiroptera	Phyllostomidae	Phyllostomus discolor	114497080
	143291	Chiroptera	Pteropodidae	Pteropus giganteus	120609356
	132908	Chiroptera	Pteropodidae	Pteropus vampyrus	105293112
	9407	Chiroptera	Pteropodidae	Rousettus aegyptiacus	107501760
	59479	Chiroptera	Rhinolophidae	Rhinolophus ferrumequinum	117035771
	29078	Chiroptera	Vespertilionidae	Eptesicus fuscus	103296377
	98922	Chiroptera	Vespertilionidae	Myotis daubentonii	132214965
	51298	Chiroptera	Vespertilionidae	Myotis myotis	118670001
	59472	Chiroptera	Vespertilionidae	Pipistrellus kuhlii	118719258
	9365	Erinaceomorpha	Erinaceidae	Erinaceus europaeus	103111473
	27675	Pilosa	Megalonychidae	Choloepus didactylus	119509908
	54180	Primates	Cercopithecidae	Trachypithecus francoisi	117086074
	9606	Primates	Hominidae	Homo sapiens	5728
	81572	Primates	Hylobatidae	Hylobates moloch	116457897
	9470	Primates	Lorisidae	Nycticebus coucang	128580539
	9785	Proboscidea	Elephantidae	Loxodonta africana	100660561
	42410	Rodentia	Cricetidae	Peromyscus eremicus	131902806
	51337	Rodentia	Dipodidae	Jaculus jaculus	101607620
TP53	494514	Carnivora	Canidae	Vulpes lagopus	121499929
	61452	Carnivora	Felidae	Neofelis nebulosa	131496929
	9691	Carnivora	Felidae	Panthera pardus	109245932
	95912	Carnivora	Hyaenidae	Hyaena hyaena	120231386
	9662	Carnivora	Mustelidae	Meles meles	123929470
	9643	Carnivora	Ursidae	Ursus americanus	123792132
	9417	Chiroptera	Phyllostomidae	Artibeus jamaicensis	119053542

89673	Chiroptera	Phyllostomidae	Phyllostomus discolor	114515376
143291	Chiroptera	Pteropodidae	Pteropus giganteus	120589680
132908	Chiroptera	Pteropodidae	Pteropus vampyrus	105291226
9407	Chiroptera	Pteropodidae	Rousettus aegyptiacus	107515689
59479	Chiroptera	Rhinolophidae	Rhinolophus ferrumequinum	117013763
29078	Chiroptera	Vespertilionidae	Eptesicus fuscus	103296897
98922	Chiroptera	Vespertilionidae	Myotis daubentonii	132218058
51298	Chiroptera	Vespertilionidae	Myotis myotis	118672084
59472	Chiroptera	Vespertilionidae	Pipistrellus kuhlii	118726809
9365	Erinaceomorpha	Erinaceidae	Erinaceus europaeus	103113788
27675	Pilosa	Megalonychidae	Choloepus didactylus	119514044
54180	Primates	Cercopithecidae	Trachypithecus francoisi	117067758
9606	Primates	Hominidae	Homo sapiens	7157
81572	Primates	Hylobatidae	Hylobates moloch	116459052
9470	Primates	Lorisidae	Nycticebus coucang	128570606
9785	Proboscidea	Elephantidae	Loxodonta africana	100663725
42410	Rodentia	Cricetidae	Peromyscus eremicus	131917260
51337	Rodentia	Dipodidae	Jaculus jaculus	101609339

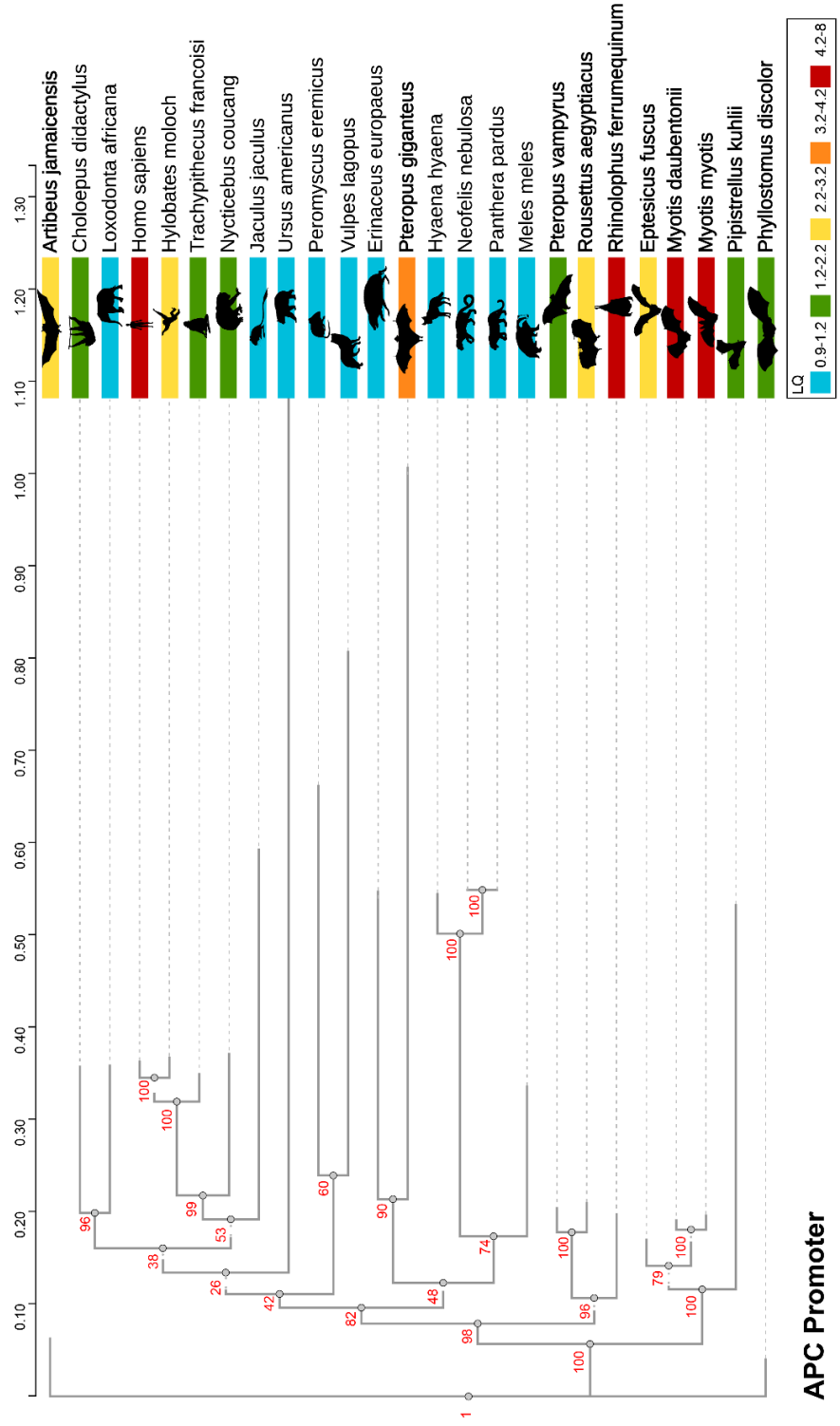

Figure S 1: Unrooted maximum likelihood tree generated by IQ−TREE constructed from the promoter region of the APC gene. Numbers above nodes represent bootstrap support and species color-coded with each respective longevity quotient.

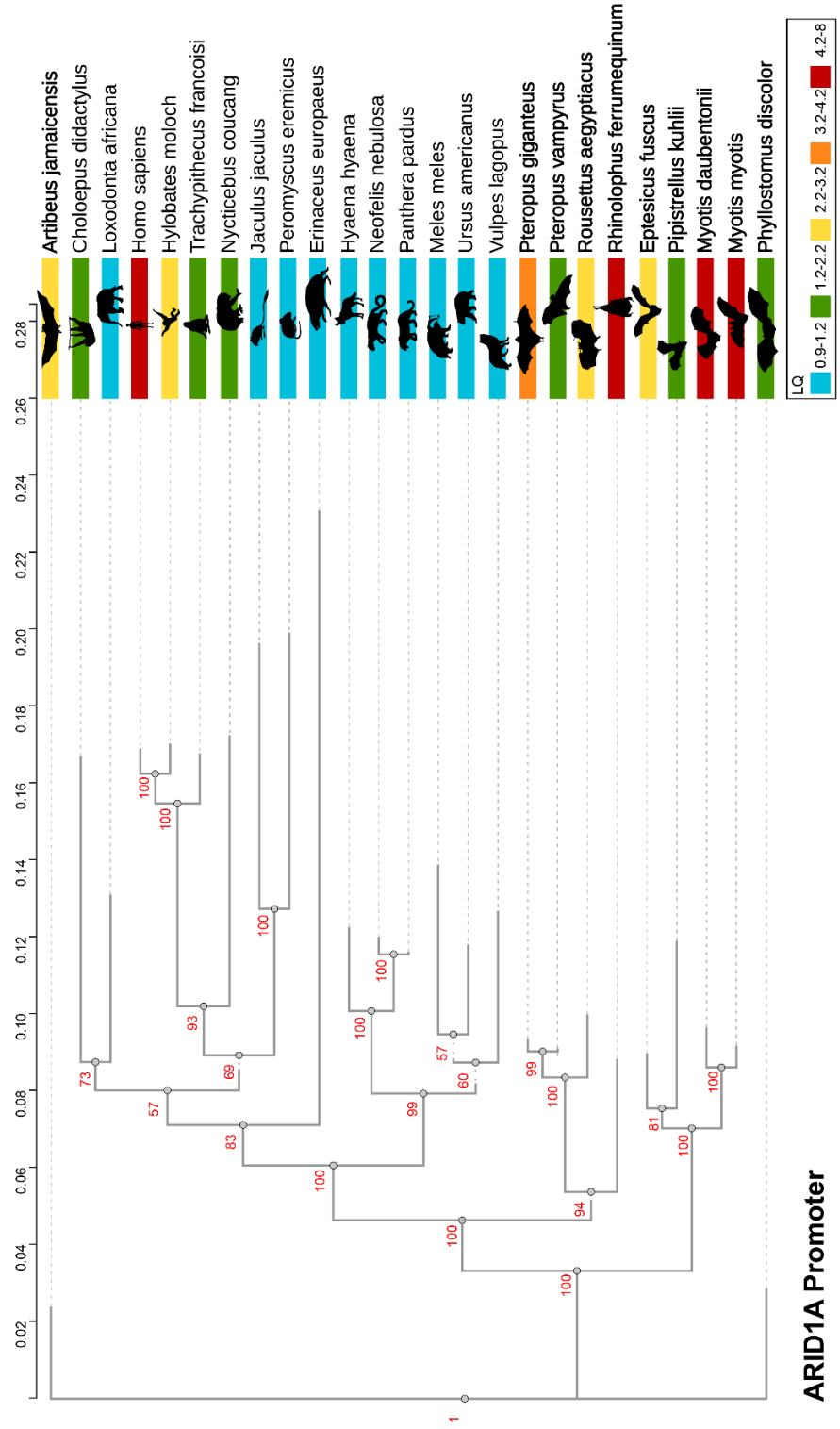

Figure S 2: Unrooted maximum likelihood tree generated by IQ−TREE constructed from the promoter region of the ARID1A gene. Numbers above nodes represent bootstrap support and species color-coded with each respective longevity quotient.

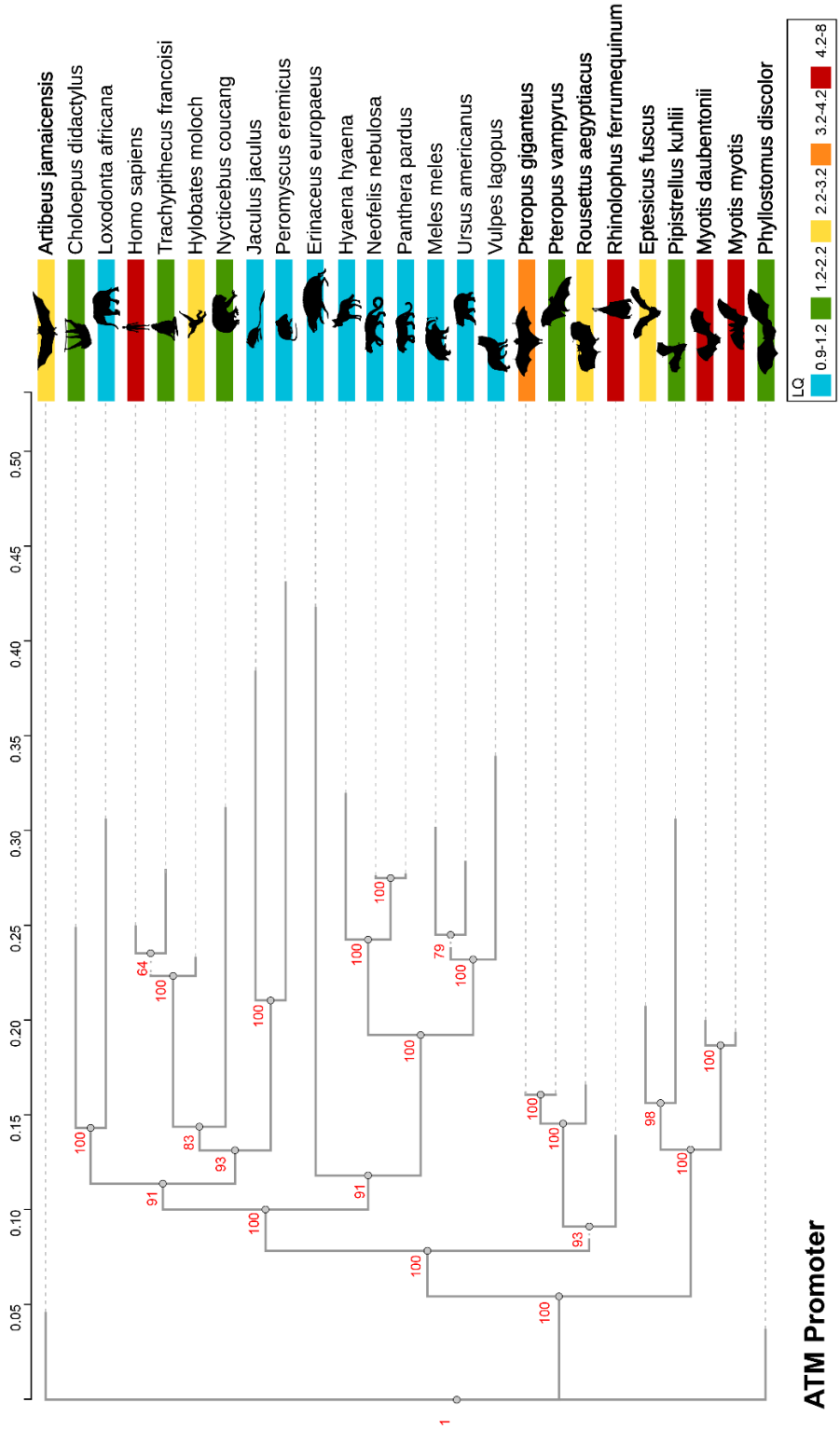

Figure S 3: Unrooted maximum likelihood tree generated by IQ−TREE constructed from the promoter region of the ATM gene. Numbers above nodes represent bootstrap support and species color-coded with each respective longevity quotient.

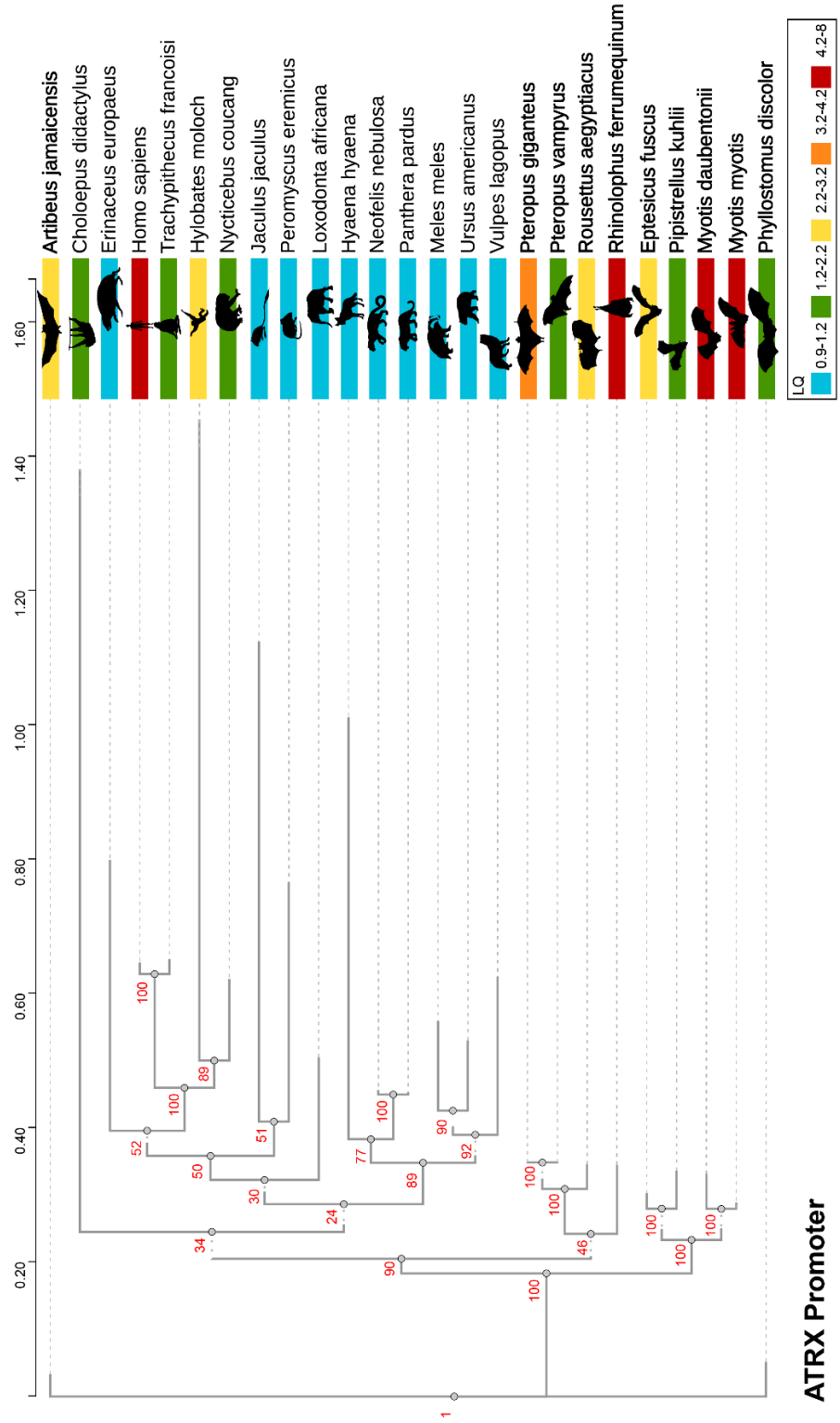

Figure S 4: Unrooted maximum likelihood tree generated by IQ−TREE constructed from the promoter region of the ATRX gene. Numbers above nodes represent bootstrap support and species color-coded with each respective longevity quotient.

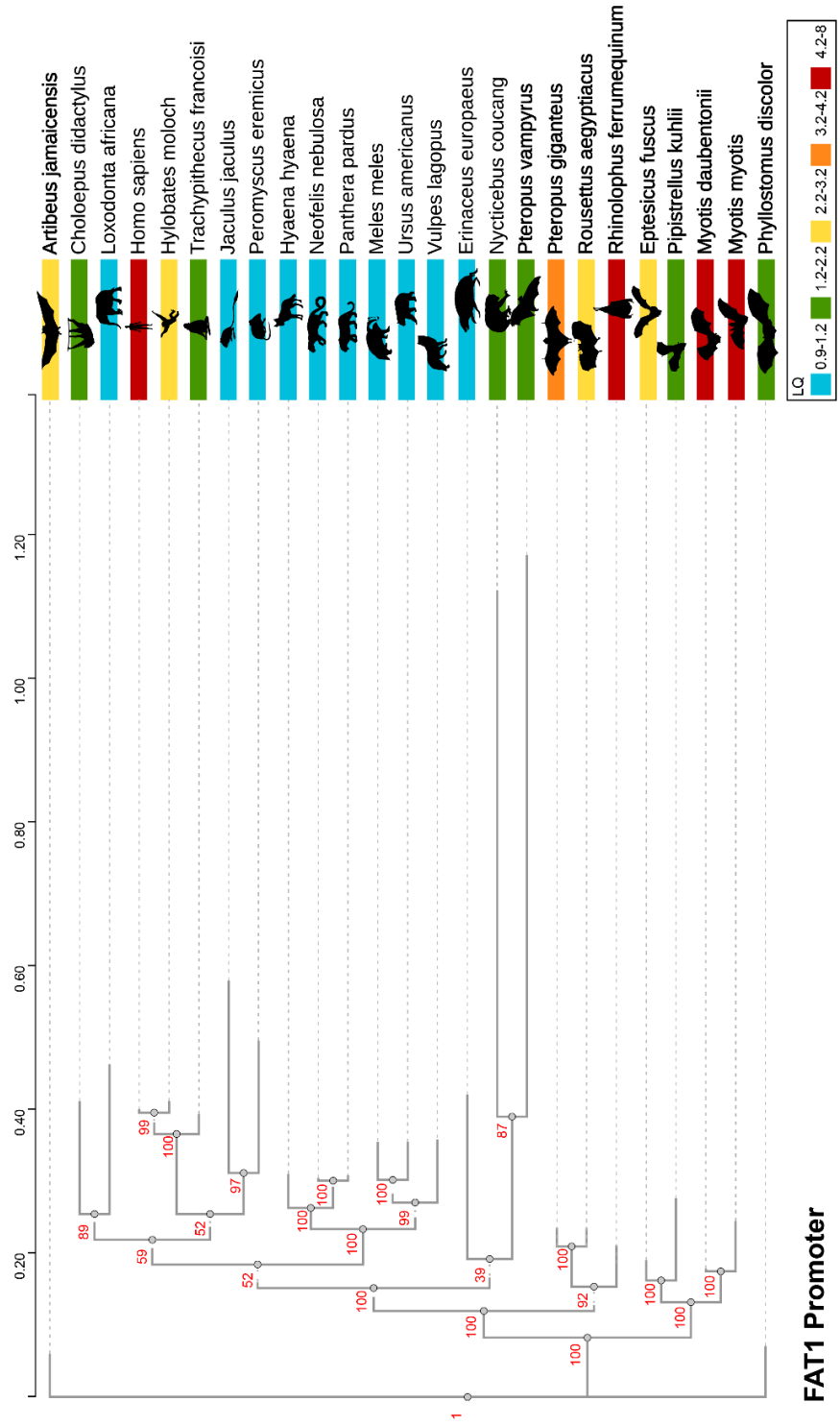

Figure S 5: Unrooted maximum likelihood tree generated by IQ−TREE constructed from the promoter region of the FAT1 gene. Numbers above nodes represent bootstrap support and species color-coded with each respective longevity quotient.

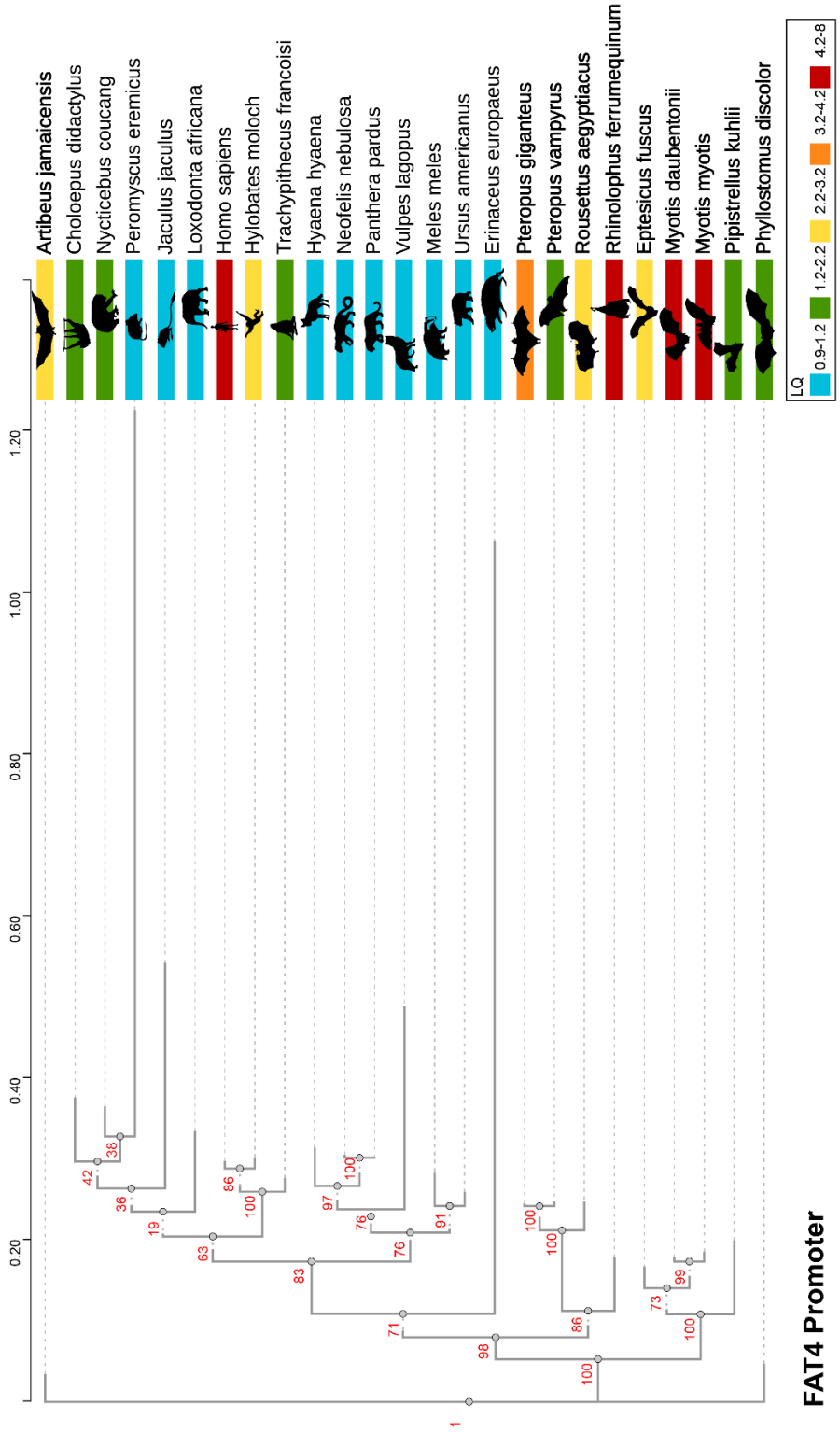

Figure S 6: Unrooted maximum likelihood tree generated by IQ−TREE constructed from the promoter region of the FAT4 gene. Numbers above nodes represent bootstrap support and species color-coded with each respective longevity quotient.

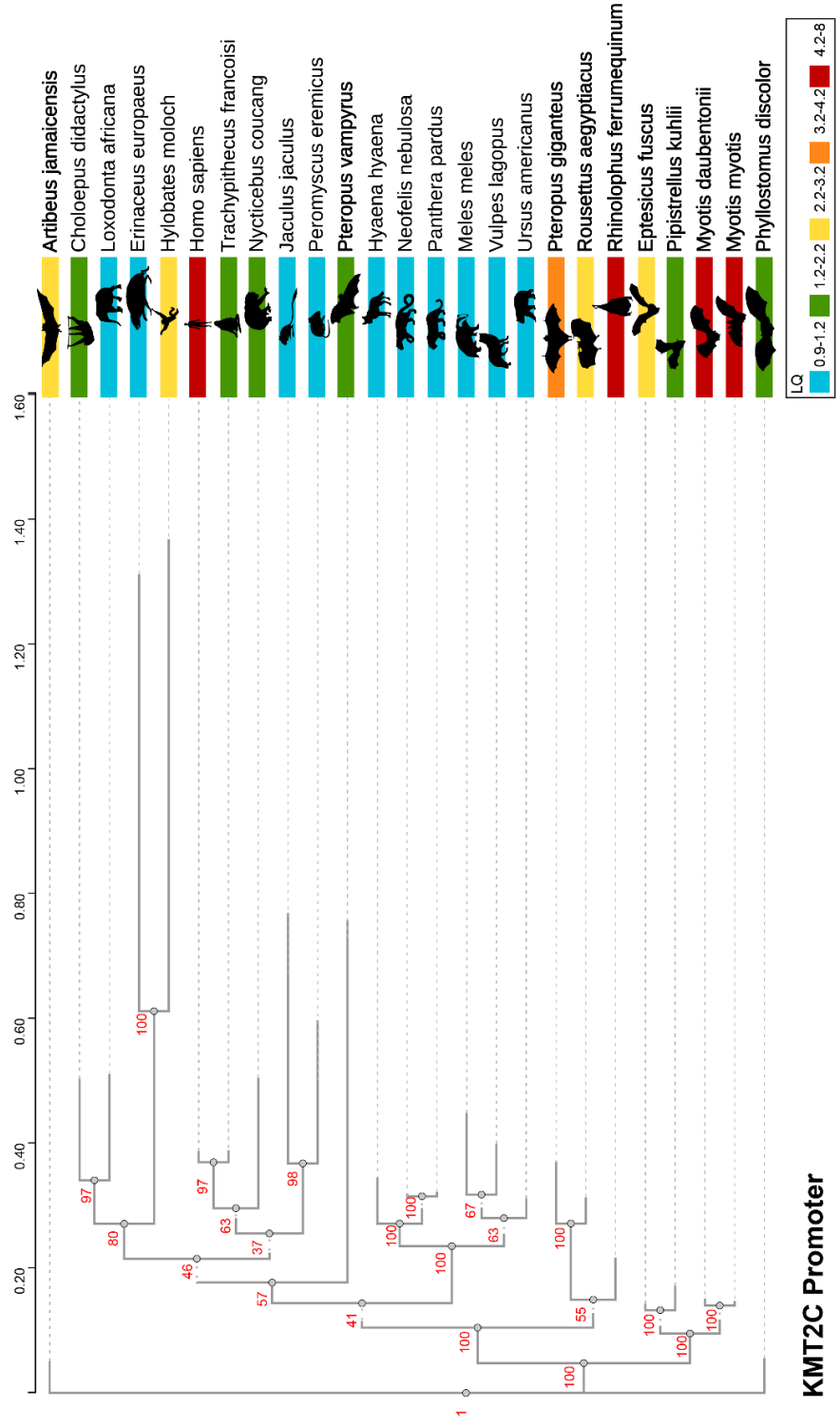

Figure S 7: Unrooted maximum likelihood tree generated by IQ−TREE constructed from the promoter region of the KMT2C gene. Numbers above nodes represent bootstrap support and species color-coded with each respective longevity quotient.

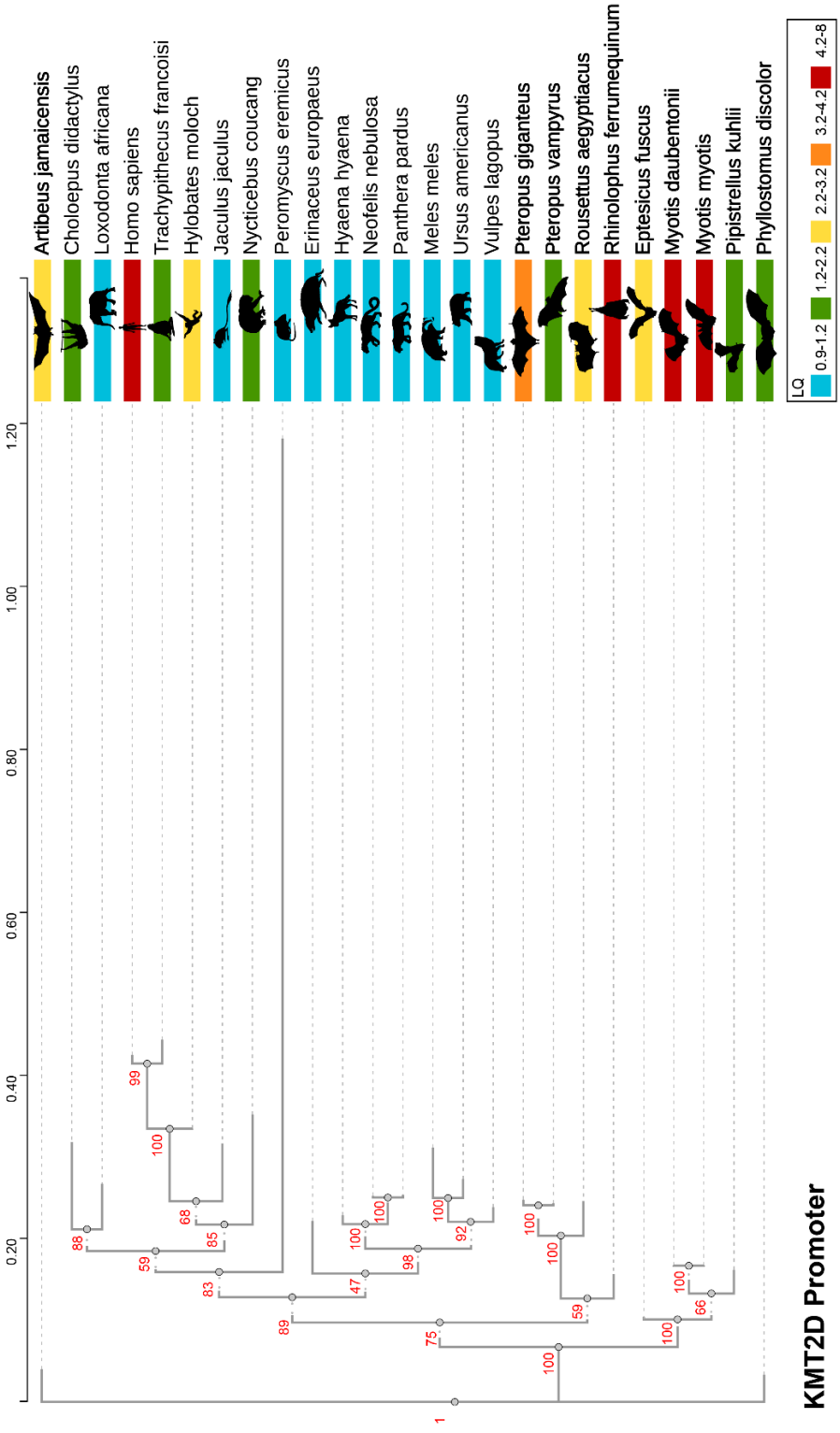

Figure S 8: Unrooted maximum likelihood tree generated by IQ−TREE constructed from the promoter region of the KMT2D gene. Numbers above nodes represent bootstrap support and species color-coded with each respective longevity quotient.

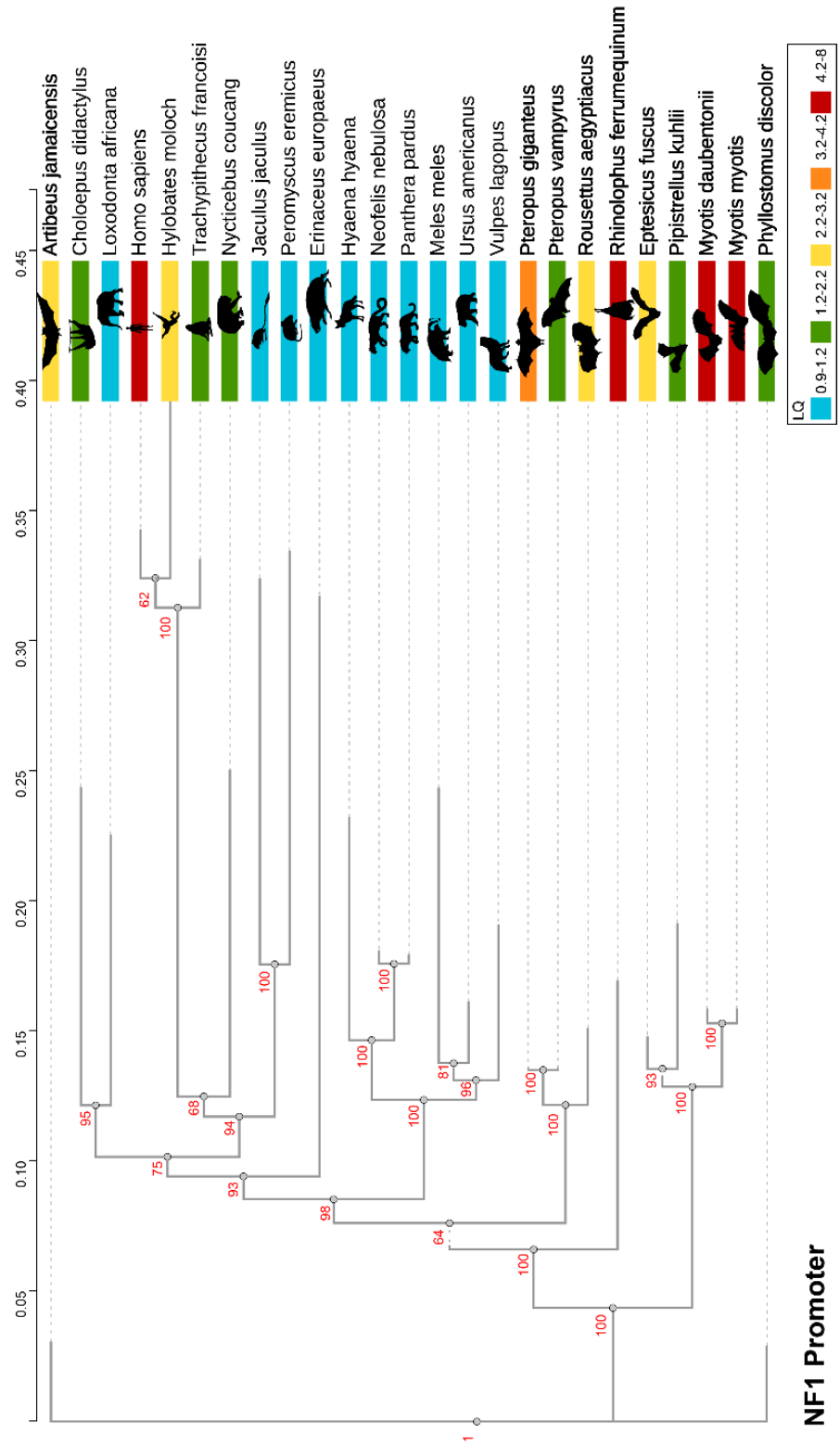

Figure S 9: Unrooted maximum likelihood tree generated by IQ−TREE constructed from the promoter region of the NF1 gene. Numbers above nodes represent bootstrap support and species color-coded with each respective longevity quotient.

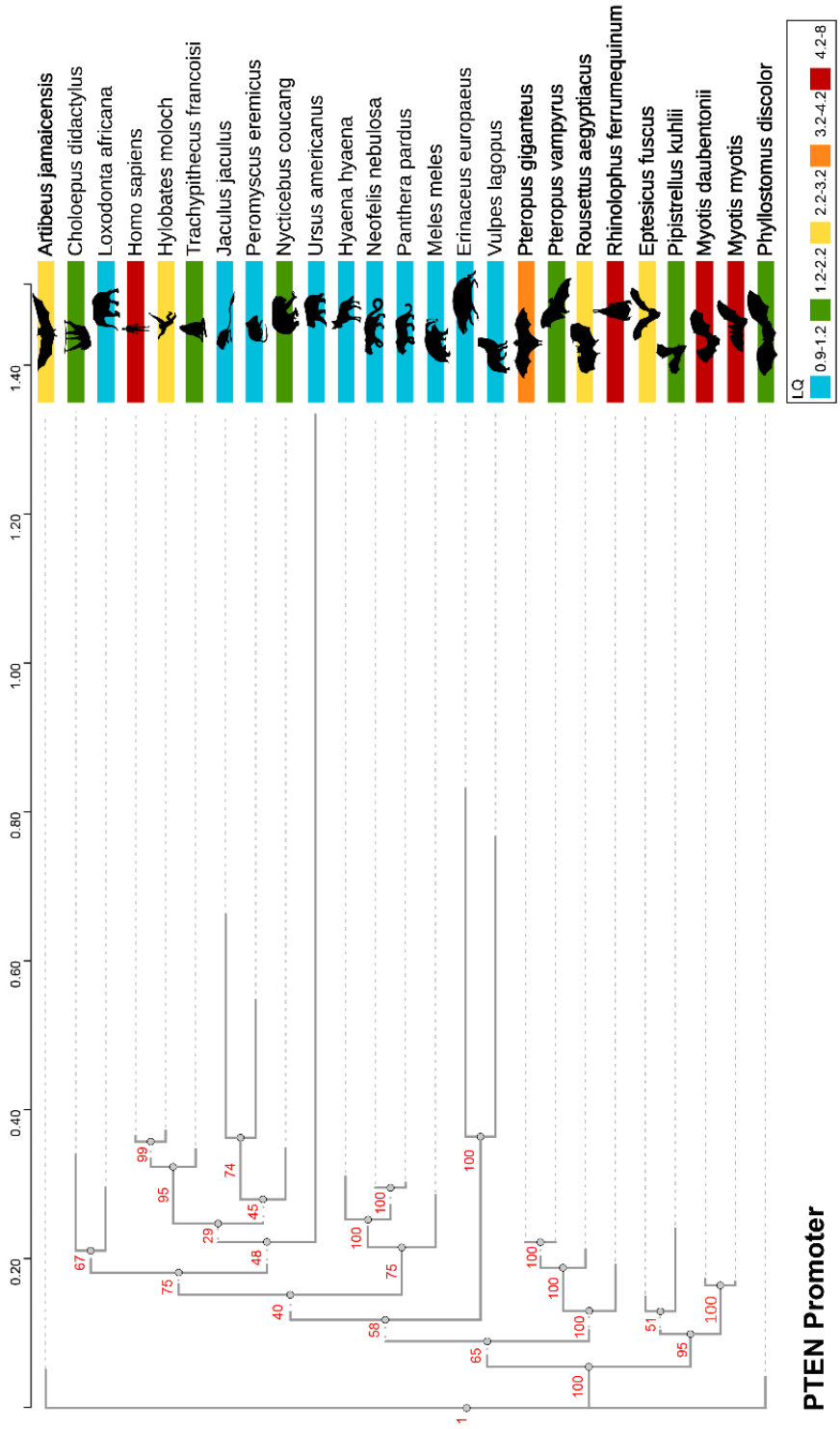

Figure S 10: Unrooted maximum likelihood tree generated by IQ−TREE constructed from the promoter region of the PTEN gene. Numbers above nodes represent bootstrap support and species color-coded with each respective longevity quotient.

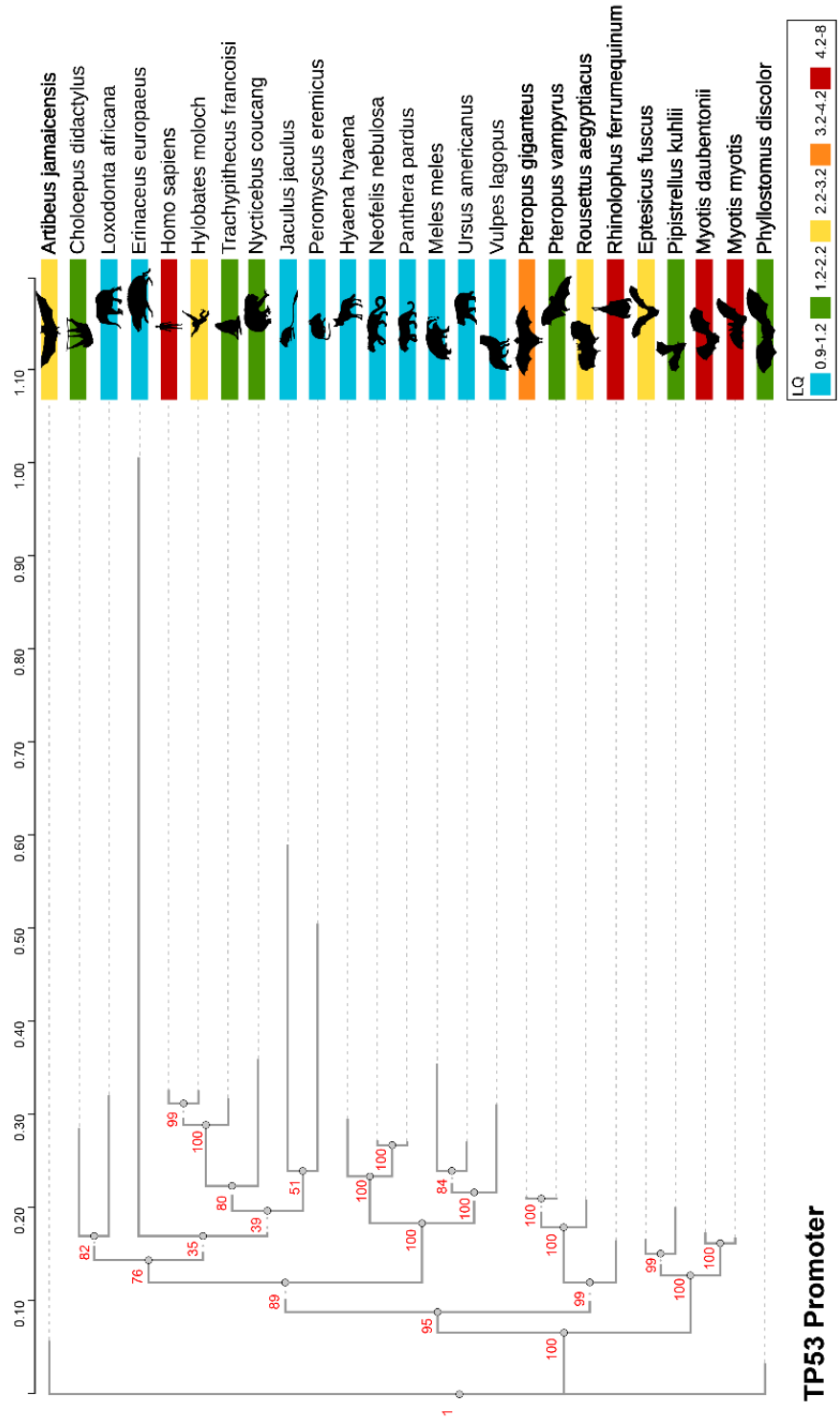

Figure S 11: Unrooted maximum likelihood tree generated by IQ−TREE constructed from the promoter region of the TP53 gene. Numbers above nodes represent bootstrap support and species color-coded with each respective longevity quotient.

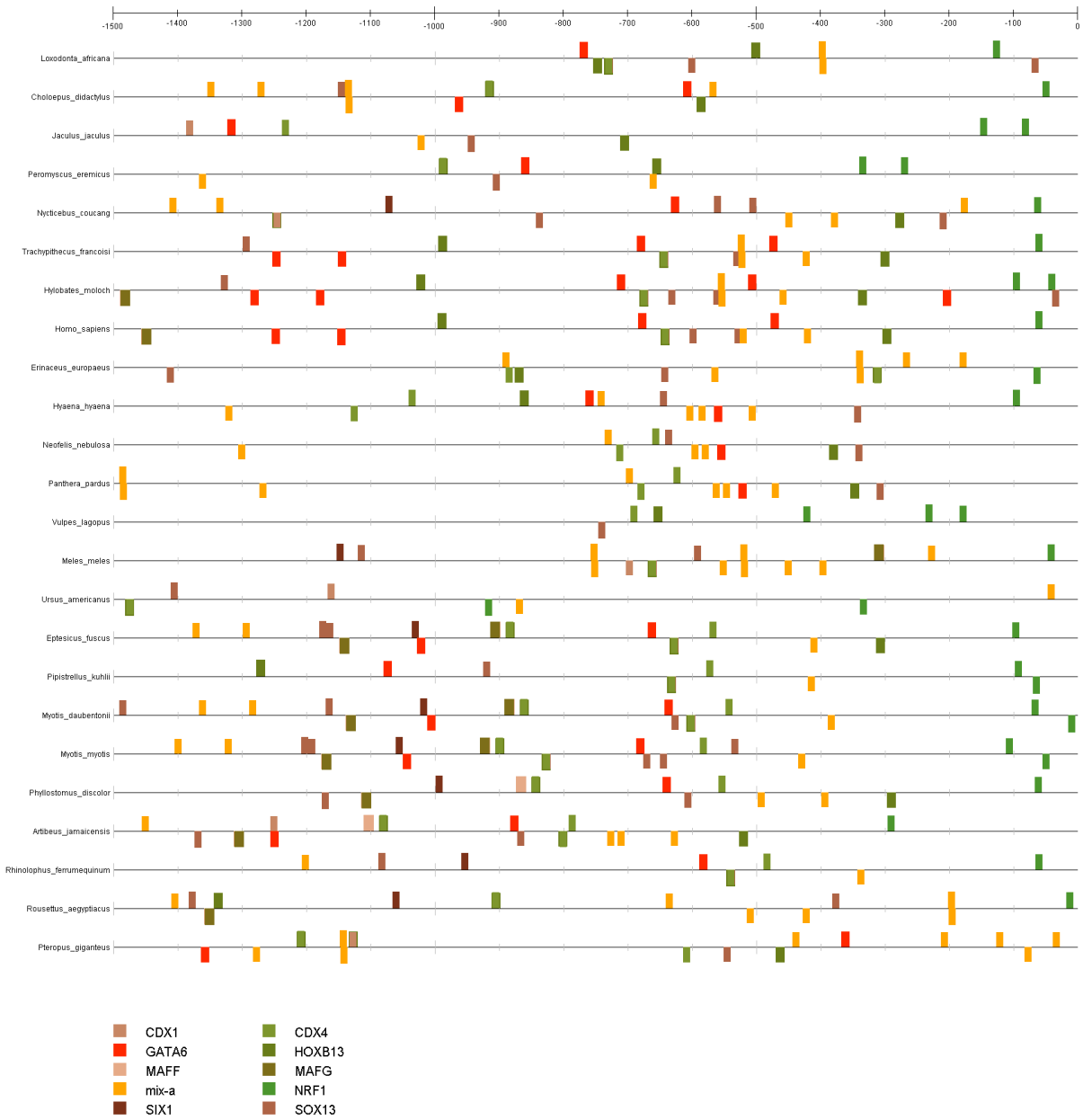

Figure S 12: Ciiider enriched predictions of transcription factors binding sites in APC promoters' sequences.

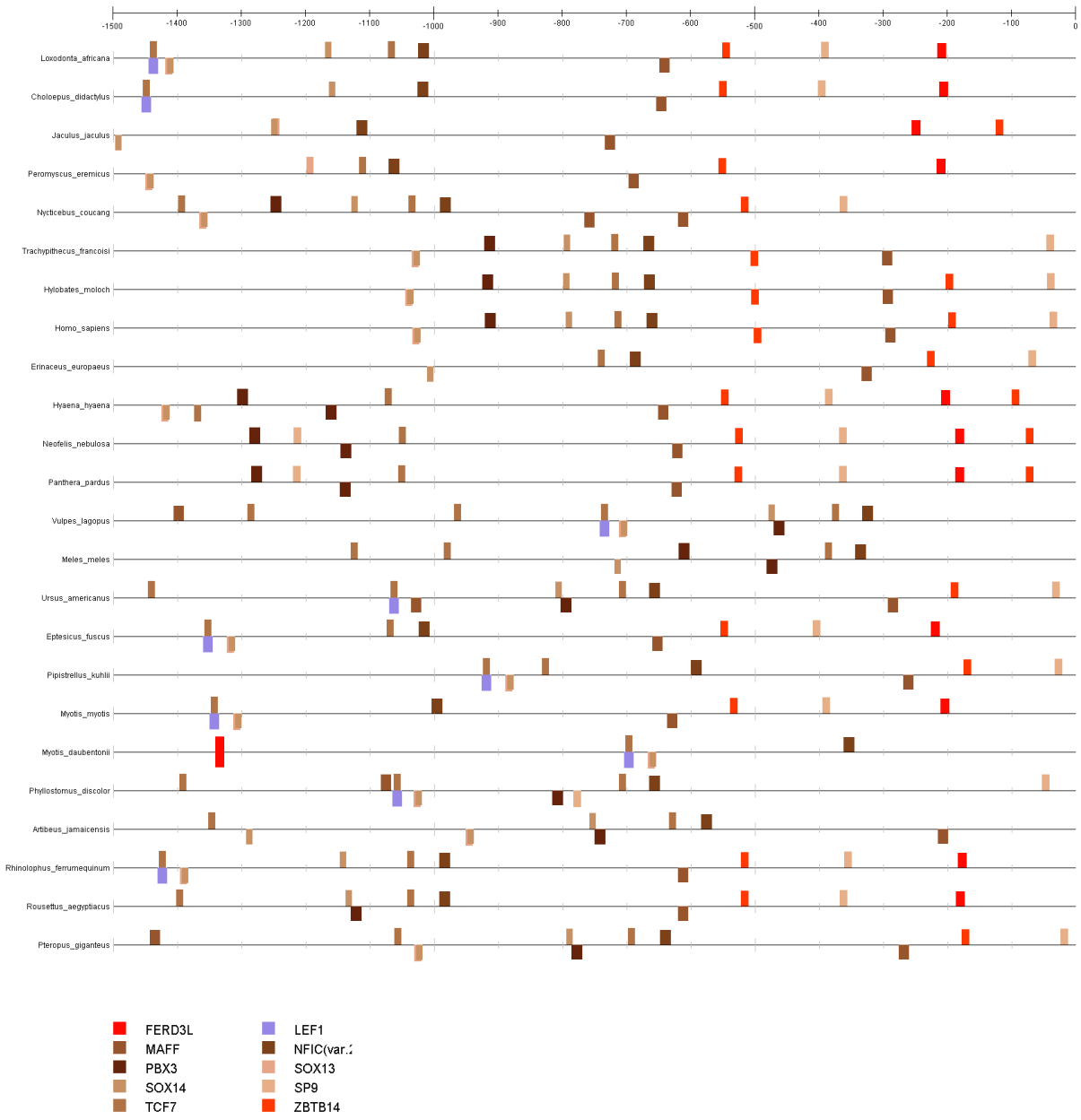

Figure S 13: Ciiider enriched predictions of transcription factors binding sites in ARID1A promoters' sequences.

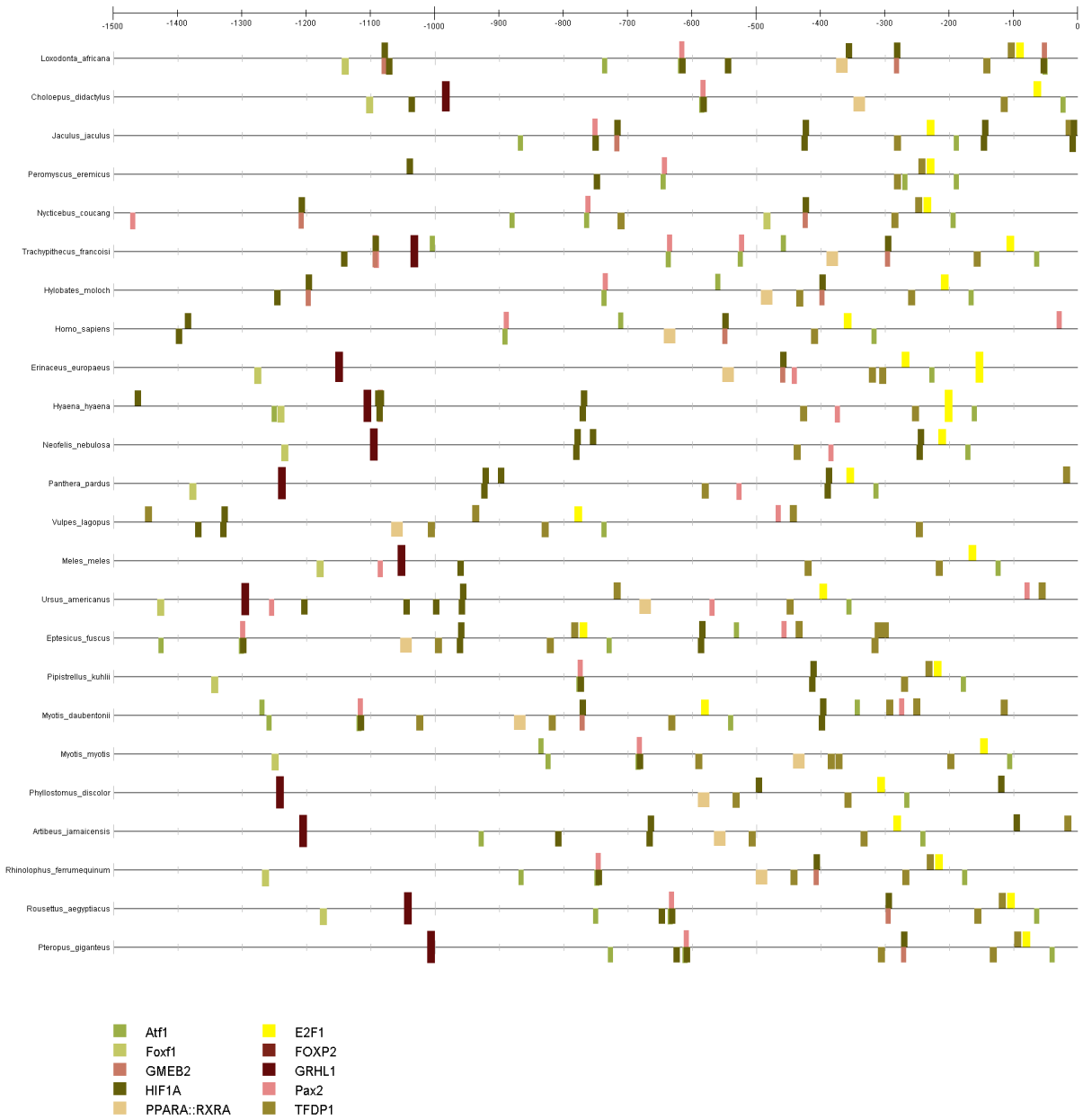

Figure S 14: Ciiider enriched predictions of transcription factors binding sites in ATM promoters' sequences.

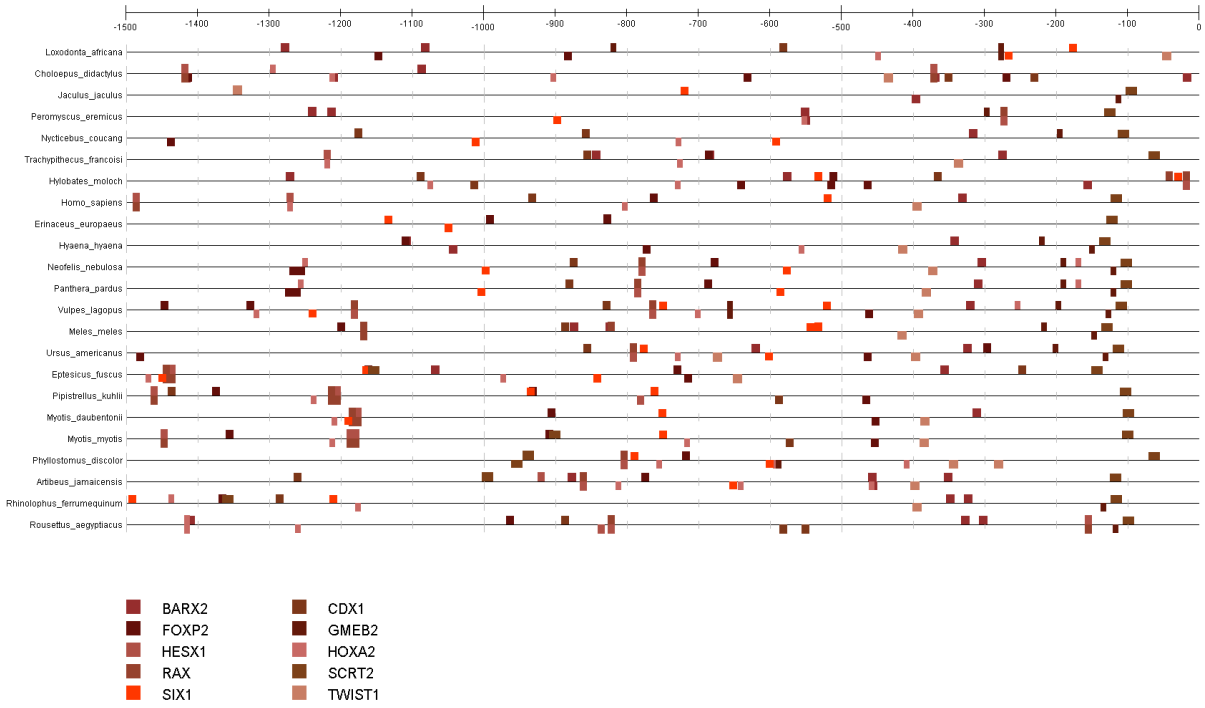

Figure S 15: Ciiider enriched predictions of transcription factors binding sites in ATRX promoters' sequences.

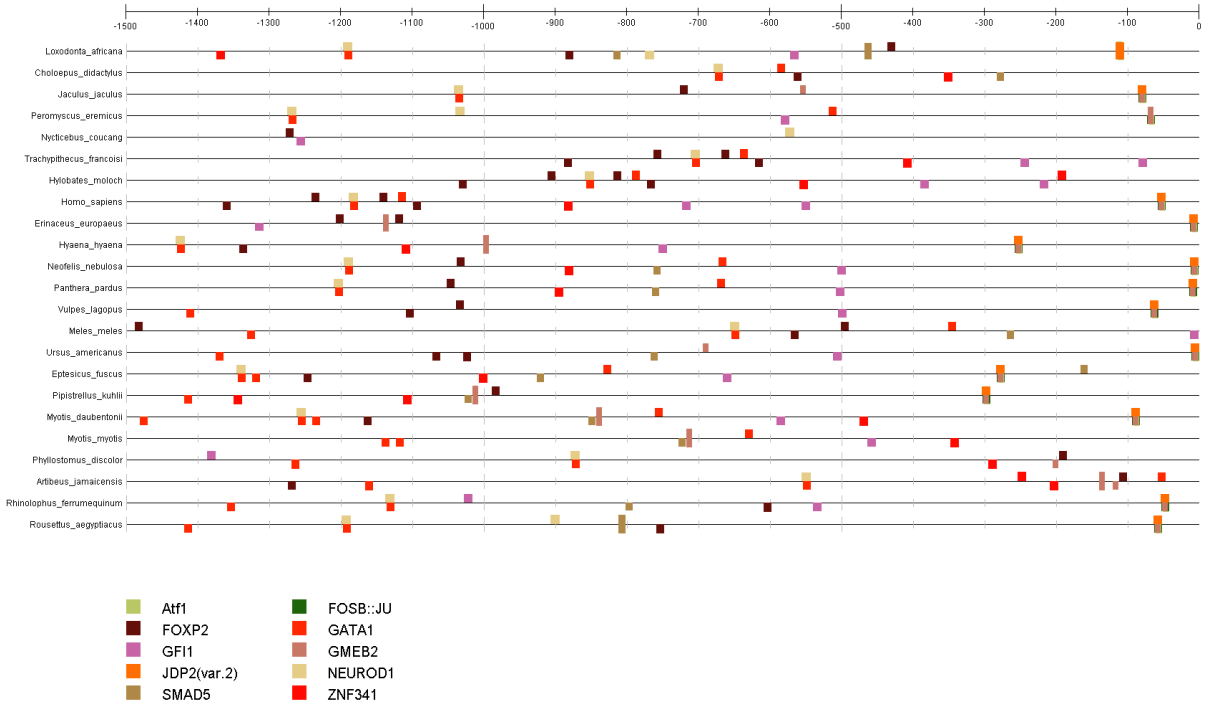

Figure S 16: Ciiider enriched predictions of transcription factors binding sites in FAT1 promoters' sequences.

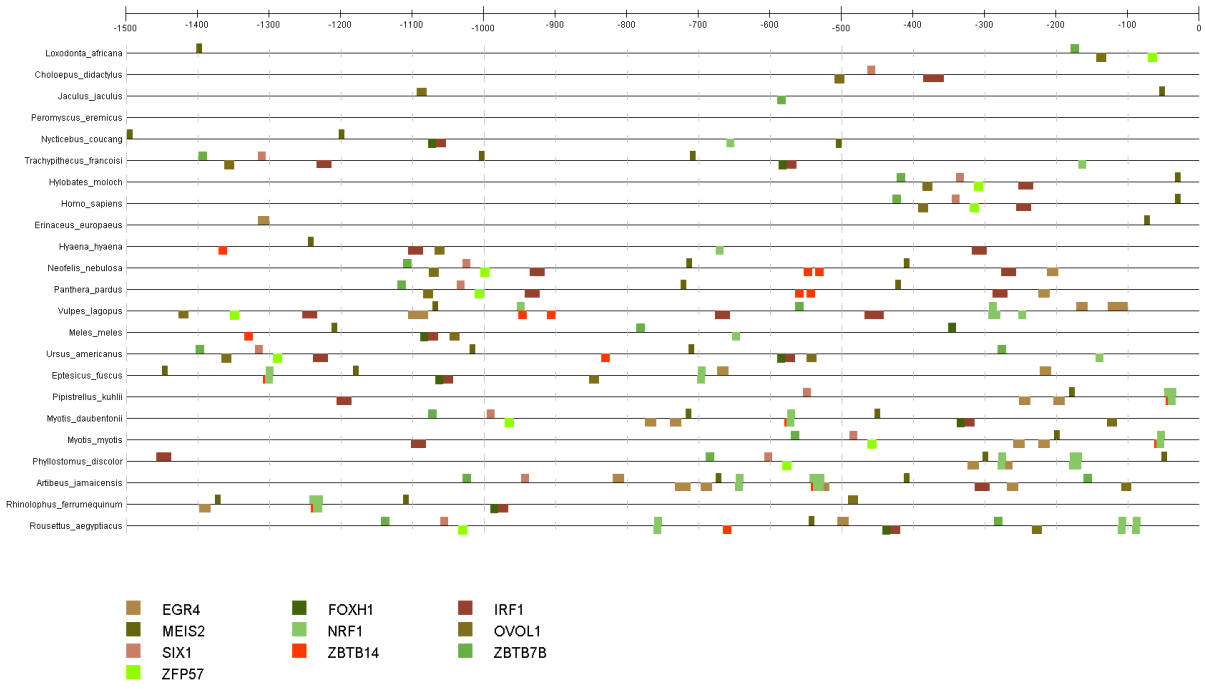

Figure S 17: Ciiider enriched predictions of transcription factors binding sites in FAT4 promoters' sequences.

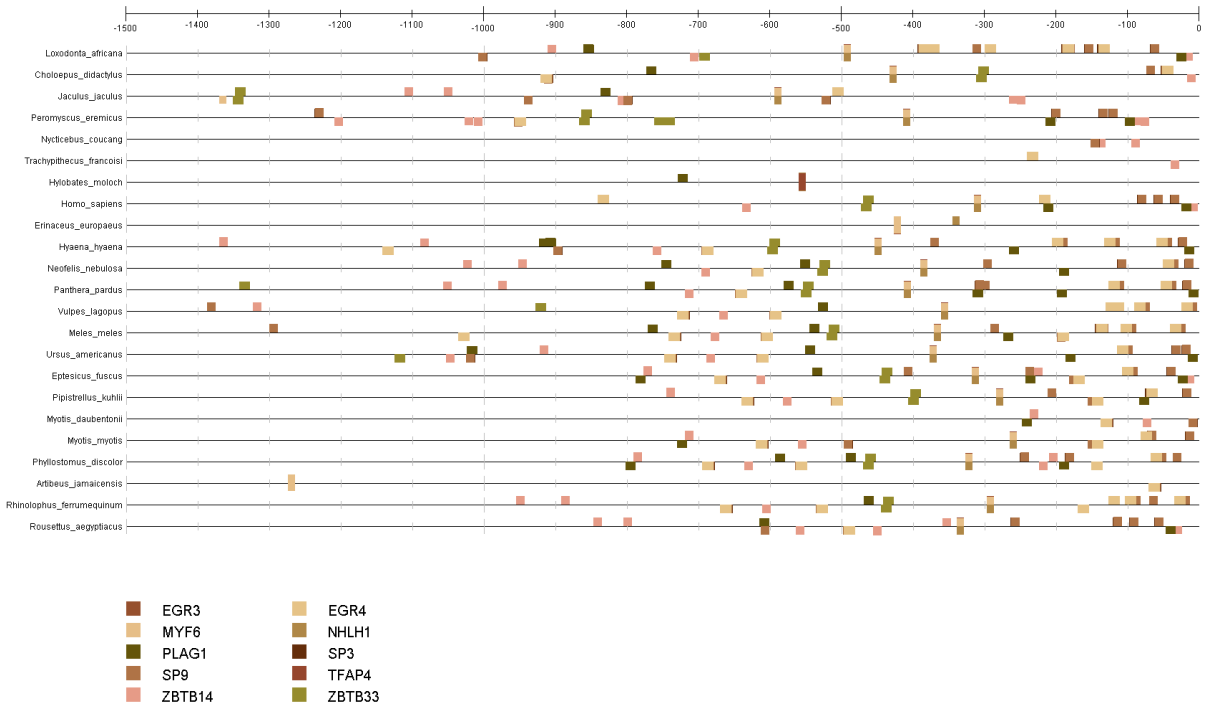

Figure S 18: Ciiider enriched predictions of transcription factors binding sites in KMT2C promoters' sequences.

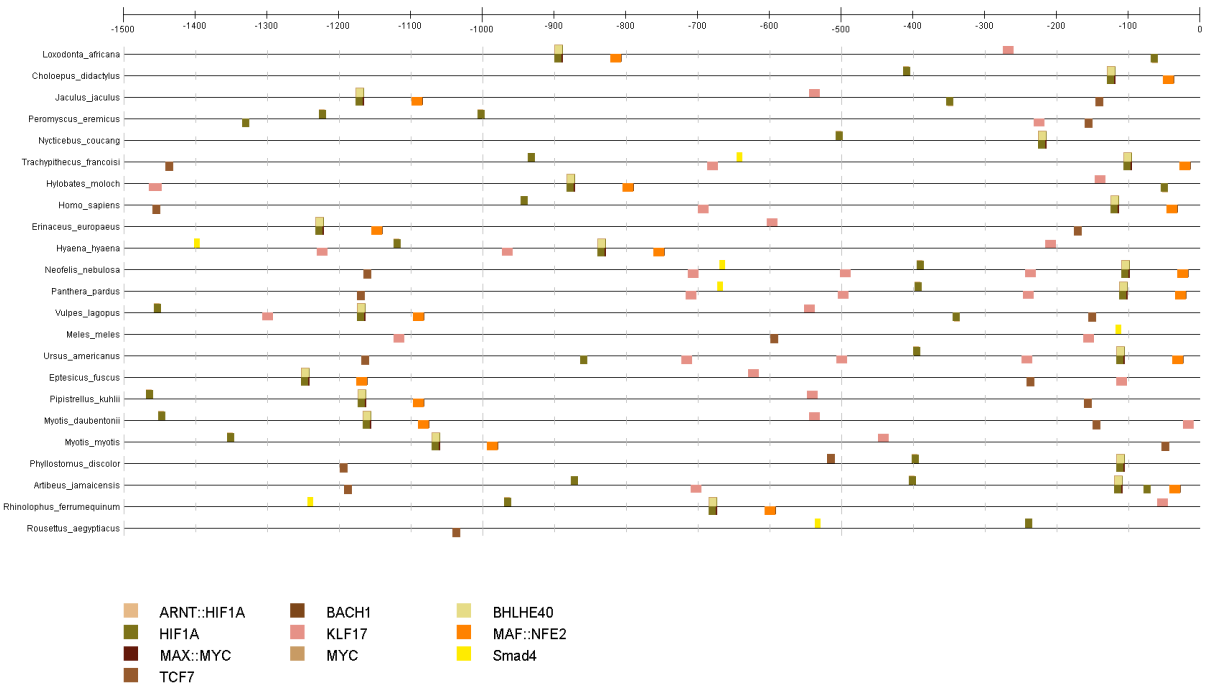

Figure S 19 Ciiider enriched predictions of transcription factors binding sites in KMT2D promoters' sequences.

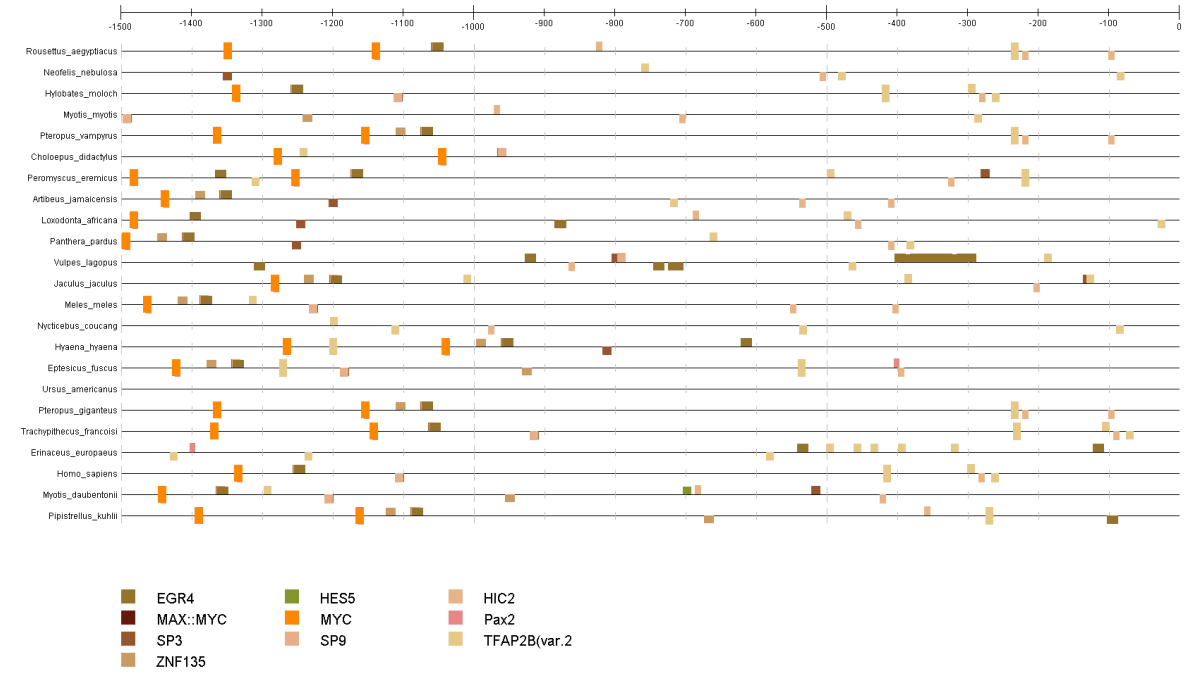

Figure S 20: Ciiider enriched predictions of transcription factors binding sites in PTEN promoters' sequences.

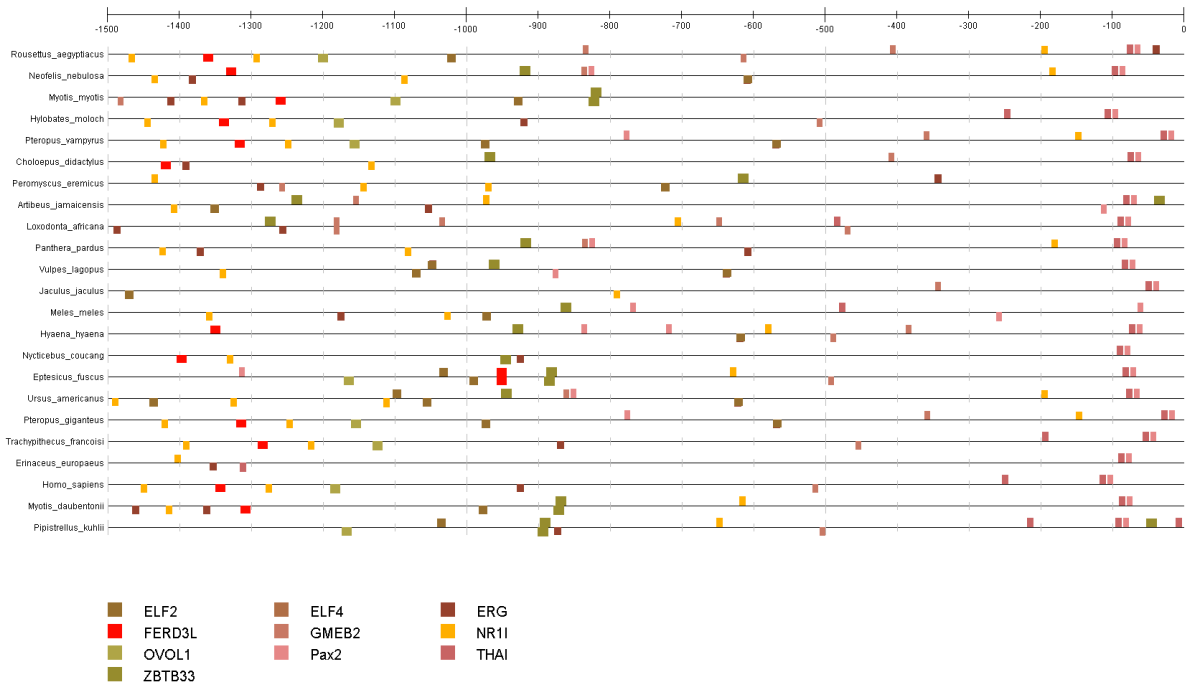

Figure S 21: Ciiider enriched predictions of transcription factors binding sites in TP53 promoters' sequences.